RECEIVED
LAWRENCE
RADIATION LABORATORY
JUN 1 1970
LIBRARY AND
DOCUMENTS SECTION

UCRL-19141

c.2

MOVING-BOUNDARY MEASUREMENTS OF TRANSFERENCE NUMBERS

Kong-Heong Tan
(M.S. Thesis)

March 1970

AEC Contract No. W-7405-eng-48

TWO-WEEK LOAN COPY

This is a Library Circulating Copy
which may be borrowed for two weeks.
For a personal retention copy, call
Tech. Info. Division, Ext. 5545

UCRL-19141
c.2

LAWRENCE RADIATION LABORATORY
UNIVERSITY of CALIFORNIA BERKELEY

DISCLAIMER

This document was prepared as an account of work sponsored by the United States Government. While this document is believed to contain correct information, neither the United States Government nor any agency thereof, nor the Regents of the University of California, nor any of their employees, makes any warranty, express or implied, or assumes any legal responsibility for the accuracy, completeness, or usefulness of any information, apparatus, product, or process disclosed, or represents that its use would not infringe privately owned rights. Reference herein to any specific commercial product, process, or service by its trade name, trademark, manufacturer, or otherwise, does not necessarily constitute or imply its endorsement, recommendation, or favoring by the United States Government or any agency thereof, or the Regents of the University of California. The views and opinions of authors expressed herein do not necessarily state or reflect those of the United States Government or any agency thereof or the Regents of the University of California.

MOVING-BOUNDARY MEASUREMENTS OF TRANSFERENCE NUMBERS

Contents

Abstract 1

I. Introduction 2

II. Theoretical Background 4

II. 1. Basic Concepts 4

II. 2. Analysis at the Boundary 6

II. 3. The Kohlrausch Function 6

II. 4. The "Volume Correction" Term 8

III. Experimental Description 16

III. 1. Overall Description 16

III. 2. Calculation of $c_3/c_o|_{x = -\infty}$ 23

III. 3. Determination of V 27

(a) Base Volume Calibration 27

(b) Volume covered by the Moving Boundary . . . 33

(i) Cell-Filling 33

(ii) Boundary Observation 38

(iii) Volume Analysis 40

III. 4. The Recording of the Time Variable, t 45

III. 5. The Recording of the Time-Averaged Current, I. . 47

III. 6. The Parameters a_B and b_B 51

III. 7. The Transference Numbers of NH_4NO_3 Solutions at 25°C 58

III. 8. The Transference Numbers of $AgNO_3$ Solutions at 25°C 62

III. 9. Summary of the Transference Number Data for NH_4NO_3 Solutions at 25°C 72

IV. Conclusions 76

V. Acknowledgments 77

Nomenclature 78

References 81

Source Material 83

MOVING-BOUNDARY MEASUREMENTS OF TRANSFERENCE NUMBERS

Kong-Heong Tan*

Inorganic Materials Research Division
Lawrence Radiation Laboratory, and
Department of Chemical Engineering
University of California, Berkeley

March 1970
(M.S. Thesis)

ABSTRACT

The moving-boundary technique as established by Milios[1] was employed to determine the transference numbers of ammonium nitrate solutions at concentrations covering both the dilute and concentrated regimes in order to render more complete its set of transport properties.

Silver nitrate was the following solution in all instances.

---

*Present address: Cambridge, Massachusetts

I. INTRODUCTION

The moving-boundary technique has received considerable attention since the initial conception of it materialized in the late 1800's. The classic review paper by MacInnes and Longsworth[2] in 1932 echoed the now widespread belief that this method is indeed superior to others in providing a reliable tool with which to investigate the transference number behavior of ions in electrolytic solutions. Since 1962, there have been a flurry of theoretical and experimental endeavors[3-6] on the subject; however, no sweeping changes have been suggested in either the procedure of boundary observation or the subsequent treatment of results.

Very recently, a significant step toward reformulating the existing method was taken by Milios,[1] with the result that an expression for the transference number that is applicable at any concentration now exists. The usefulness of the expression depends, to some extent, on the degree of accuracy present when the density of the following solution is assumed to be linearly related to its concentration over the range of interest. The fact that this range can be experimentally minimized for such a representation between the density and concentration to be justified prompts one to believe that a theoretically valid and experimentally accessible technique is at hand.

The present effort describes the application of the Milios technique to the determination of the cation transference numbers of dilute and concentrated ammonium nitrate solutions at 25°C, as a contributive part

in an active attempt[7] to collect transport property data of electrolytes to strengthen existing theoretical interpretations as well as suggest new approaches.

The particular experimental set-up designed yields not only accurate data for ammonium nitrate, but also good numbers for silver nitrate, the following solution used.

II. THEORETICAL BACKGROUND

II.1. Basic Concepts

The moving-boundary system and the corresponding nomenclature that Milios[1] engineered is closely followed in all aspects of the present work. The reader is referred to his thesis for the overall descriptions of the two-salt system.

In order for a cohesive argument to be presented, however, the necessary background equations are briefly reiterated.

They are, the continuity equation in one-dimensional form,

$$\frac{\partial c_i}{\partial t} = -\frac{\partial c_i v_i}{\partial x} \quad , \tag{1}$$

a current density-flux expression,

$$i = F\sum_i z_i c_i v_i \quad , \tag{2}$$

a mathematical statement of electroneutrality,

$$\sum_i z_i c_i = 0 \quad , \tag{3}$$

and a transport equation in one-dimensional form,

$$c_i \frac{\partial \mu_i}{\partial x} = RT \sum_j \frac{c_i c_j}{c_T \mathcal{D}_{ij}} (v_j - v_i) \quad . \tag{4}$$

When the motion of the ions is referred to that of the solvent, the transference number (relative to the solvent velocity) is defined as

that fraction of the current carried by an ion in a solution of uniform composition, and that is, for a solution of two ions,

$$t_+ = \frac{z_+c_+(v_+-v_0)}{z_+c_+(v_+-v_0)+z_-c_-(v_--v_0)} \tag{5}$$

or, in terms of the transport properties $\mathcal{D}_{ij}$,

$$t_+ = \frac{z_+\mathcal{D}_{+0}}{z_+\mathcal{D}_{+0}-z_-\mathcal{D}_{-0}} \quad . \tag{6}$$

II.2. Analysis at the Boundary

At the two-salt boundary, an analysis that is similar to that of Weber[8] but that involves transport equation (4) (applicable for dilute as well as concentrated solutions) along with the others mentioned produces the following exact relationships,

$$t_1 = \frac{F}{i} z_3 \frac{c_3}{c_0}\bigg|_{x=-\infty} [c_0(v_0 - v_b)] \tag{7}$$

and

$$t_2 = \frac{F}{i} z_3 \frac{c_3}{c_0}\bigg|_{x=+\infty} [c_0(v_0 - v_b)] \quad . \tag{8}$$

Here, v_b represents the boundary velocity, the subscript $x = -\infty$ necessitates that the term it is attached to be evaluated in solution A far above the boundary (see Fig. 1), and $x = +\infty$ indicates that treatment of its parent term must be done in solution B far below the boundary.

This derivation is effected by noting that the system is in a steady state in a coordinate frame which is moving with the boundary velocity v_b. The reader is referred to Milios' thesis for the complete derivation and to the subsequent paper by Milios and Newman[9] for further discussions.

II.3. The Kohlrausch Function

Equations (7) and (8), when manipulated correctly, yield an expression for the Kohlrausch regulating function

$$\frac{t_1}{t_2} = \frac{c_3/c_0|_{x=-\infty}}{c_3/c_0|_{x=+\infty}} \quad ,$$

about which much has been said in the literature. MacInnes and Longsworth[2] in their review paper in 1932 presented the most detailed picture of

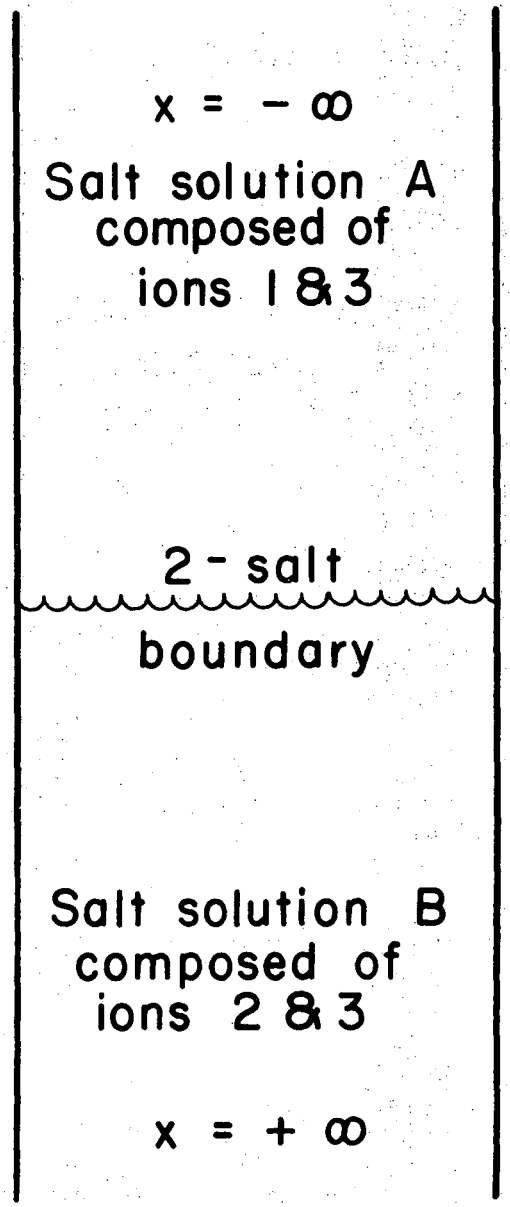

XBL679-5222

Fig. 1. The 2-salt boundary. (Reproduced from Milios' thesis for illustrative purposes.)

this function. For a vertical channel, as it is almost certain that the concentration of the adjusted or regulated solution immediately following the leading solution at the boundary is different from the original following solution; a concentration boundary is necessarily set up and left behind as the two-salt boundary progresses along the channel. At this point, it is interesting to note that optical observation of such concentration boundaries was possible as early as 1944, with the aid of a Schlieren scanning technique.[10]

II.4. The "Volume Correction" Term

In order that the term v_0 in Equation (4) and (8) can be determined, the scheme presented in Fig. 1 must be enlarged to include the closed electrode chamber. Hence, the reader is referred to Fig. 2., which depicts this arrangement with the two-salt boundary and concentration boundary included. This is done so that volume variations at the chosen electrode can be followed and assessed.

The Milios approach involves letting the electrode reaction be that of anodic metal dissolution, with the boundaries progressing up the channel, and then calculating for v_0 by means of material balances over the region below a plane x fixed in the solvent, allowances being made for the dissolution of the anode, the concentration dependence of the density of B, and the transference of ions across the solvent plane.

Specifically, the volume V_0 bounded by the electrode and by the plane x moving with the solvent velocity v_0, changes with time as

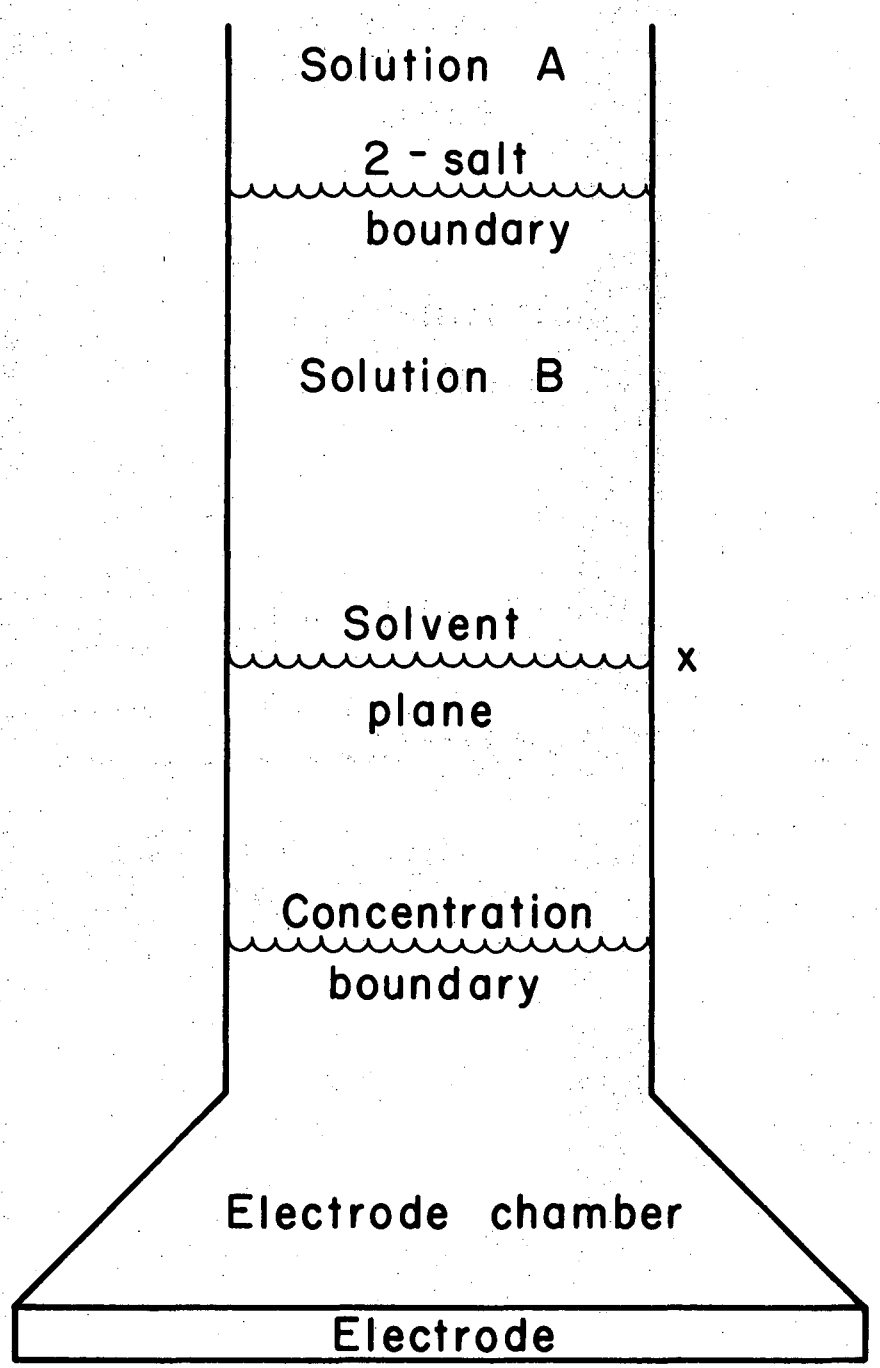

XBL679-5223

Fig. 2. The closed electrode. (Reproduced from Milios' thesis for illustrative purposes.)

$$\frac{dV_0}{dt} = \frac{d}{dt}\int_{V_0} dV = -v_0 A - \frac{I}{z_+ F}\frac{M_e}{\rho_e} \tag{9}$$

where A = channel cross-sectional area

I = total current passing through channel (negative for an anode)

M_e = atomic weight of the anode

and ρ_e = density of the anode.

Hence the two contributions to the volume rate are, respectively, the displacement of the solvent plane and the volume rate of dissolution of the anode. As the solvent mass in V_o remains invariant, a material balance on it produces the following equation,

$$\frac{d}{dt}\int_{V_0} c_0 dV = 0 \tag{10}$$

As for the electrolyte, a material balance gives

$$\frac{d}{dt}\int_{V_0} c_+ dV = \frac{It_+}{z_+ F} - \frac{I}{z_+ F} \tag{11}$$

The two terms describe, respectively, the transport of cations across the solvent plane and the contribution of cations as a result of the anodic dissolution process.

At this point, an assumption is made to enhance the theoretical and practical desirability of the transference number expression, namely, that

$$\rho_B = \alpha_B + \beta_B c_B \tag{12}$$

below the solvent plane at x. But an exact expression for ρ_B is available, that is,

$$\rho_B = M_B c_B + M_B \; c_{OB} \tag{13}$$

Therefore,

$$c_{OB} = a_B + b_B c_B = a_B + b_B \frac{c_+}{\nu_+^B} \tag{14}$$

and

$$a_B = \alpha_B / M_o \tag{15}$$

$$b_B = (\beta_B - M_B) / M_o \quad . \tag{16}$$

Equation (10) then becomes

$$a_B \frac{d}{dt} \int_{V_o} dV + \frac{b_B}{\nu_+^B} \frac{d}{dt} \int_{V_o} c_+ dV = 0 \quad , \tag{17}$$

or

$$a_B \; v_O A + \frac{a_B I}{z_+ F} \frac{M_e}{\rho_e} - \frac{b_B}{\nu_+^B} \frac{I}{z_+ F} (t_+ - 1) = 0 \tag{18}$$

with the introduction of Equations (9) and (11).

Therefore,

$$v_O = - \frac{i}{F} \left[\frac{M_e}{z_+ \rho_e} + \frac{1 - t_+}{z_+ \nu_+^B} \frac{b_B}{a_B} \right] \quad . \tag{19}$$

This can be rewritten as

$$v_0 = -\frac{i}{F}\left[\frac{M_e}{z_2\rho_e} + \frac{1-t_2^B}{z_2\nu_2}\frac{b_B}{a_B}\right] \tag{20}$$

as ion 2 is the cation reacting at the anode.

Finally, an explicit expression for the transference number of ion 1, the leading ion, is obtained through Equations(7) and (8), with the result that

$$t_1 = -a_B\frac{z_3c_3}{c_0}\Bigg|_{x=-\infty}\left[\frac{FV}{It} + \frac{M_e}{z_2\rho_e} + \frac{b_B}{z_2\nu_2a_B}\right] \tag{21}$$

where V is the volume through which the boundary moves when current I is passed for time t.

It is evident that the validity of this equation hinges heavily upon the degree of approximation of the density assumption made.

It is therefore imperative that this degree of approximation be ascertained. The trend in the literature on the question of the representation of density - concentration relationships suggests the following, in the manner first shown by Root,

$$\rho = k_1 + k_2c + k_3c^{3/2} + k_4c^2 \quad . \tag{22}$$

Equation (13) points out that in general,

$$\rho_i = M_ic_i + M_o c_o \quad . \tag{23}$$

Therefore,

$$c_o = e + fc_i + gc_i^{3/2} + hc_i^2 \tag{24}$$

where $e = k_1/M_o$; $f = (k_2 - M_i)/M_o$

$$g = k_3/M_o \quad ; \quad \text{and } h = k_4/M_o \tag{25}$$

rather than Eq. (12).

A least-squares fit of Eq. (23) to yield accurate values of a and b in Equation (12) over a concentration range of c_{final} to $c_{initial}$ in the region between the solvent plane at x and the closed anode yields the following,

$$a = e - \frac{1}{2} gc_i^{3/2}\left[1 + \frac{3}{4}\epsilon + \frac{1}{80}\epsilon^2 + O(\epsilon^3)\right] - hc_i^2(1+\epsilon+\frac{1}{6}\epsilon^2) \tag{26}$$

and

$$b = f + \frac{3}{2} gc_i^{1/2}\left[1 + \frac{1}{4}\epsilon + O(\epsilon^2)\right] + 2hc_i(1 + \frac{1}{2}\epsilon) \tag{27}$$

where O indicates the order of neglected terms and $\epsilon = (c_{final} - c_{initial}) / c_{initial}$

It can easily be shown that ϵ need not be determined very accurately for a (and hence t_1) to be satisfactorily evaluated. The terms involving g and h, merely correction terms, are small compared with e and f, and the approximation is well justified.

When one realizes that a vertical channel arrangement necessarily introduces a concentration boundary dictated by the Kohlrausch

regulating function, one is forced to take into consideration this phenomenon in the specification of ϵ, in addition to that present as a result of the anodic reaction. The latter effect has been estimated by treating the anode as a vertical electrode with free convection, viz.,

$$\epsilon_1 = \frac{1.62}{c}\left(\frac{It_-}{z_+\nu_+FDA_e}\right)^{0.8}\left(\frac{\nu DL}{g\beta}\right)^{0.2} \tag{28}$$

$$\approx \frac{0.00932}{c}\left(\frac{I}{z_+\nu_+A_e}\right)^{0.8}\left(\frac{L}{\beta}\right)^{0.2} \quad . \tag{29}$$

Here, in the simplified expression,

I = the current in mAmps.

A_e = the effective electrode area in cm^2

c = the concentration in moles/liter

L = the effective electrode height in cm.

and $\beta\left(= \frac{1}{\rho}\frac{\partial\rho}{\partial c}\right)$ = the coefficient of expansion in liters/mole.

This expression is based on values of 10^{-5} cm^2/sec for D, the diffusion coefficient, 0.5 for t-, the transference number, $10^{-2}cm^2$/sec for ν, the kinematic viscosity, and 10^3cm /sec^2 for g, the gravitational acceleration term.

With regard to ϵ_2, the contribution brought about by the concentration boundary's presence, it is desirable to render this as small as experimentally possible, although as stated earlier the accuracy of a does not hinge heavily upon the means by which the ϵ's are estimated.

It is useful, then, to establish guidelines for the consideration of these two contributions to ϵ.

(i) When the initial concentration of the following solution is less than that dictated by the Kohlrausch function, an undesirable situation experiment-wise, one might add, c in Equations (26)and (27) is to be taken to be this initial value, with ϵ equal to either ϵ_1 in the anode chamber or ϵ_2 across the concentration boundary, whichever is larger. The undesirability, evidently, arises (for the present case of a rising boundary in a vertical channel) as a result of an inherent gravitational effect on the denser adjusted solution which finds itself above a less dense initially-prepared solution.

(ii) On the other hand, when the initially-prepared solution is higher in concentration than the adjusted one, one can, with little error, take c to be the concentration of the initially-prepared solution (rather than the lowest concentration of solution B present) and ϵ to be the sum of the two contributions, ϵ_1 and ϵ_2.

The choice of a vertical anode arrangement over that involving a horizontal electrode results from the fact that an appreciably smaller value for ϵ_1 is produced. This is so because with a vertical electrode there is a tendency toward uniformity in concentration in the anode chamber, whereas with a horizontal electrode layers of solution form above it with very little mixing. The values for a and b are then more accurately known (as the correction terms are smaller) and of course one is faced with a better value for the transference number.

III. Experimental Description

III. 1. Overall Features

The system, NH_4NO_3-$AgNO_3$, was studied optically at 25°C with an electrophoresis apparatus (model 238) produced by the Perkin-Elmer Corporation of Norwalk, Connecticut. Silver nitrate was the following solution in all instances. The objectives are primarily the transference numbers of ammonium nitrate solutions of various concentrations, and secondarily, those of silver nitrate. The transference number expression points out the fact that the leading ion transference number is more accurately determined, since the term $c_3/c_0\big|_{x=-\infty}$ is accurately known, whereas the term $c_3/c_0\big|_{x=+\infty}$ must be evaluated, in the present endeavor, by Rayleigh interferometry techniques. The uncertainty in the concentration term so determined reduces the accuracy of the transference number value for the following ion.

The Perkin-Elmer instrument has been described in great detail by Chapman.[11] In particular, the Rayleigh interferometry technique is well covered in his dissertation. It suffices, then, to mention just a few of the features of the Schlieren scanning technique, an optical system which is also a part of this apparatus.

A schematic drawing on the operation of the Schlieren system is depicted in Figure 3.

When the tungsten filament lamp is selected for Schlieren analyses, the entrance slit is shifted into position at the focal plane of the lens L3. A flat mirror is positioned in the optical path to deflect light from the source onto the slit. Light emerging from the slit is collimated by the lens and directed onto the flat mirror after

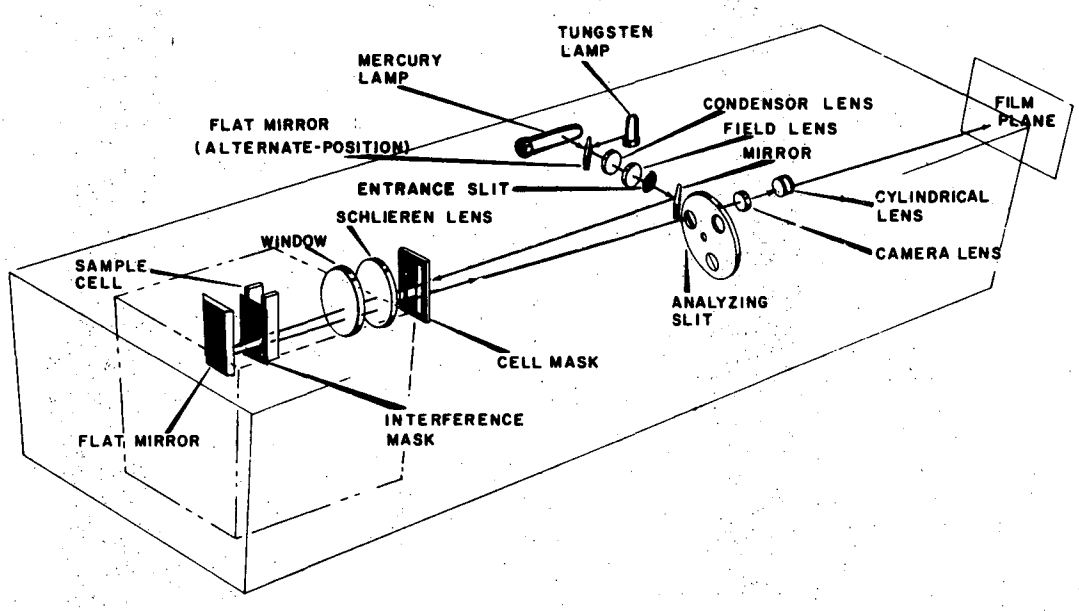

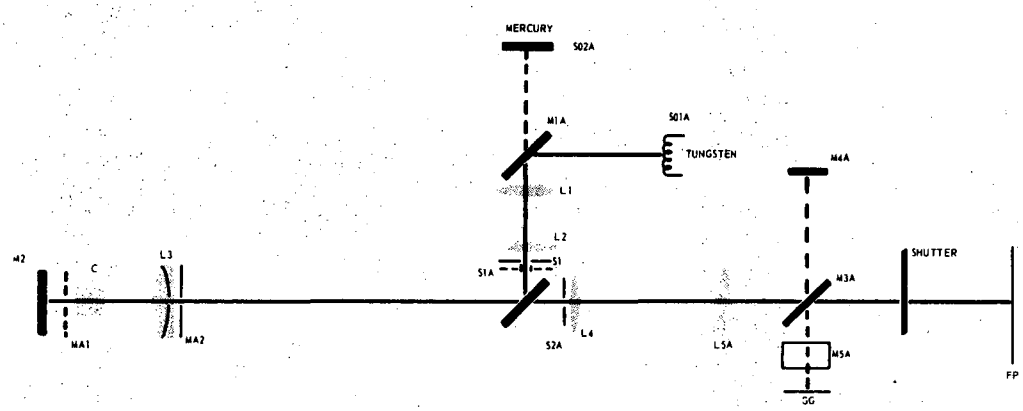

S01A - TUNGSTEN LAMP
S02A - MERCURY ARC LAMP
M1 - DIAGONAL MIRROR
M1A - DIAGONAL MIRROR (USED WITH S01 ONLY)
M2 - FLAT MIRROR IN TANK
M3A - DIAGONAL MIRROR (USED WITH VIEWING SCREEN ONLY)
M4A - FOCUSING MIRROR FOR VIEWING SCREEN IMAGE
M5A - HORIZONTAL MIRROR (USED WITH VIEWING SCREEN ONLY)
L1 - CONDENSOR LENS

L2 - FIELD LENS
L3 - SCHLIEREN LENS
L4 - CAMERA LENS
L5A - CYLINDRICAL LENS
S1 - SCHLIEREN ENTRANCE SLIT
S1A - MULTIPLE POINT SOURCE ENTRANCE SLIT (FOR RAYLEIGH FRINGES ONLY)
S2A - ANALYZER DIAPHRAGM (DIAGONAL SLIT 180° PHASE PLATE OR OPEN DIAPHRAGM)

MA1 - INTERFERENCE MASK (FOR RAYLEIGH FRINGES ONLY)
MA2 - CELL MASK
GG - GROUND GLASS VIEWING SCREEN
SHUTTER - SHUTTER FOR FILM HOLDER OR CAMERA BACK
FP - FILM PLANE
C - TISELIUS CELL

NOTE: COMPONENTS BEARING THE SUFFIX A, E. G. M1A, CAN BE MOVED IN AND OUT OF THE OPTICAL SYSTEM WITH FRONT PANEL CONTROLS.

XBL 703-467

Fig. 3. Layout of optical system. (Reproduced from Perkin Elmer Model 238 Manual.)

passing through a Tiselius[12] cell. A collimated beam is reflected from M2 through the cell and refocused by the lens to form an image of the source slit on the upper end of the analyzer diaphragm. The location of the slit image is the position of the undeviated rays which have not been deflected by gradients within the cell. Mirror M2 has adjustments in both the vertical and horizontal planes so that the image of the entrance slit can be accurately positioned across the analyzing or "diagonal" slit. This slit, normally set at a 45° angle, can be manually turned to alter the angle of inclination to compensate for excessively high or low concentrations. The analyzing slit intersects the image of the entrance slit at an angle. Any portion of the collimated beam which is diverted by a boundary in the Tiselius cell will produce additional images of the entrance slit somewhere below the undeviated position. Vertical displacement of the deviated images results in a corresponding horizontal displacement of the intersection of the image and the analyzing slit, because of the angle of the slit.

The camera lens, L4, directly behind the analyzing slit, images the cell in the film plane. When a boundary in the cell diverts a portion of the collimated beam, the deflection caused by the analyzing slit is magnified in the horizontal direction by the cylindrical lens, L5a, and the corresponding portion of the cell is displaced on one side.

The change in refractive index is not abrupt but varies throughout the boundary layers. The resulting pattern on the film takes the form of a curve which represents the rate of change in refractive index with respect to a change in cell height across the boundary.

The Tiselius cell and chambers with the corresponding electrodes are pictured in Figs. 4, 5, and 6 for convenience.

The standard chamber bottle supplied by Perkin-Elmer was modified to hold a grooved flange. The silver anode was cemented to a similarly-grooved glass-top, through a length of tubing attached to the bottom of the piece, with Silastic 892-RTV adhesive sealant purchased from Dow-Corning Corp., Midland, Michigan. The exterior of the chamber-top carries a vertical side-arm with a built-in stopcock. High vacuum silicone lubricant from Dow-Corning was used on the stopcock.

The experimental procedures are similar to those used by Milios. The pertinent features as described in his thesis apply also to the present work. It is the intention, however, to give a detailed description; consequently elaborations on the techniques employed in the several stages will be made.

For the present system, the transference number expression takes the following form.

$$t_1 = a_B \left.\frac{c_3}{c_o}\right|_{x=-\infty} \left[\frac{FV}{It} + \frac{M_e}{\rho_e} + \frac{b_B}{a_B}\right] \tag{30}$$

where subscript 1 refers to the ammonium ion

3 refers to the nitrate ion

0 refers to the solvent, water

B refers to the silver nitrate following solution

e refers to the silver anode

and $|x = -\infty$ indicates that the term so categorized must be evaluated in the ammonium nitrate solution rather than in the silver nitrate solution.

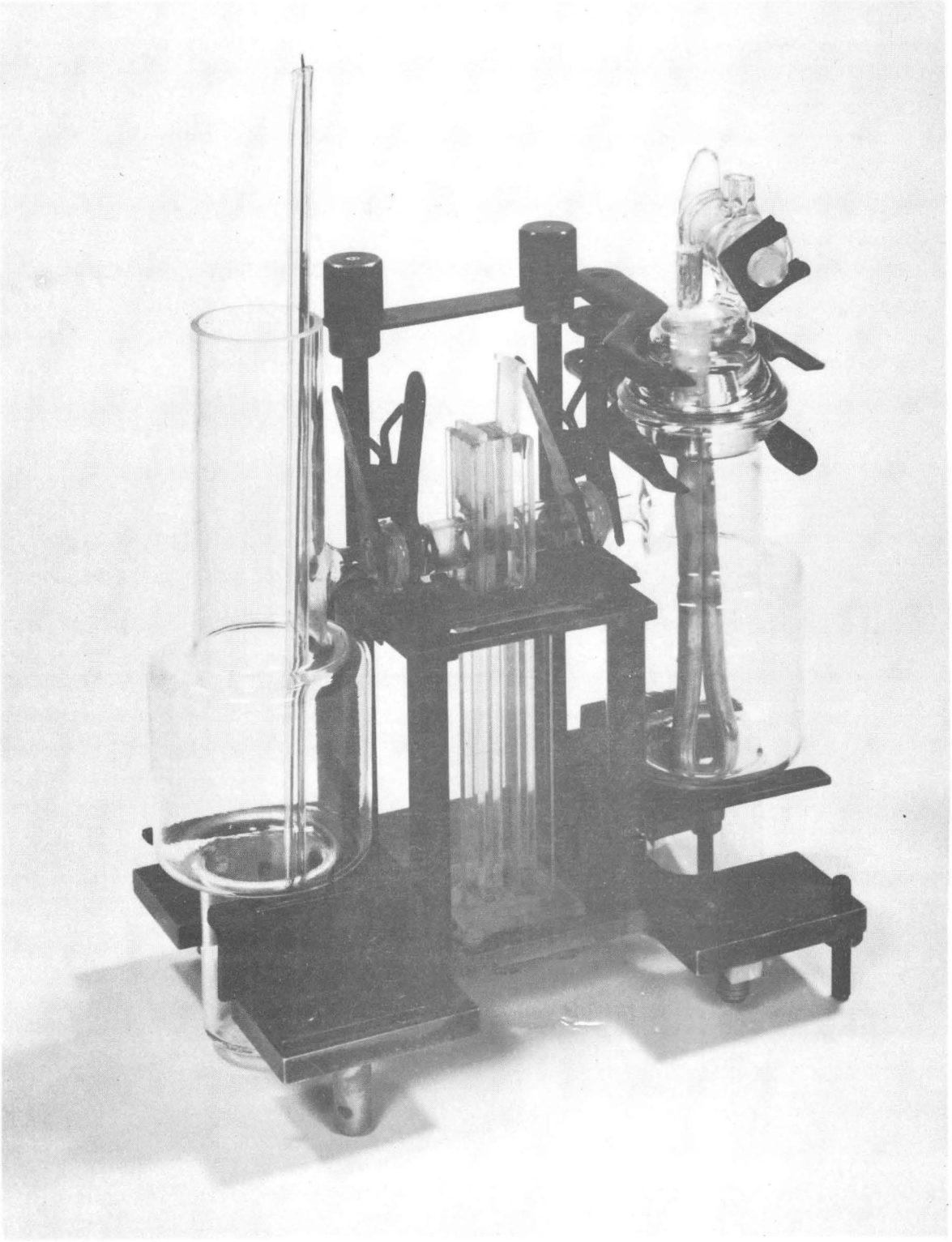

XBB 679-5169

Fig. 4. Tiselius cell in holder. (Reproduced from Milios' thesis for illustrative purposes.)

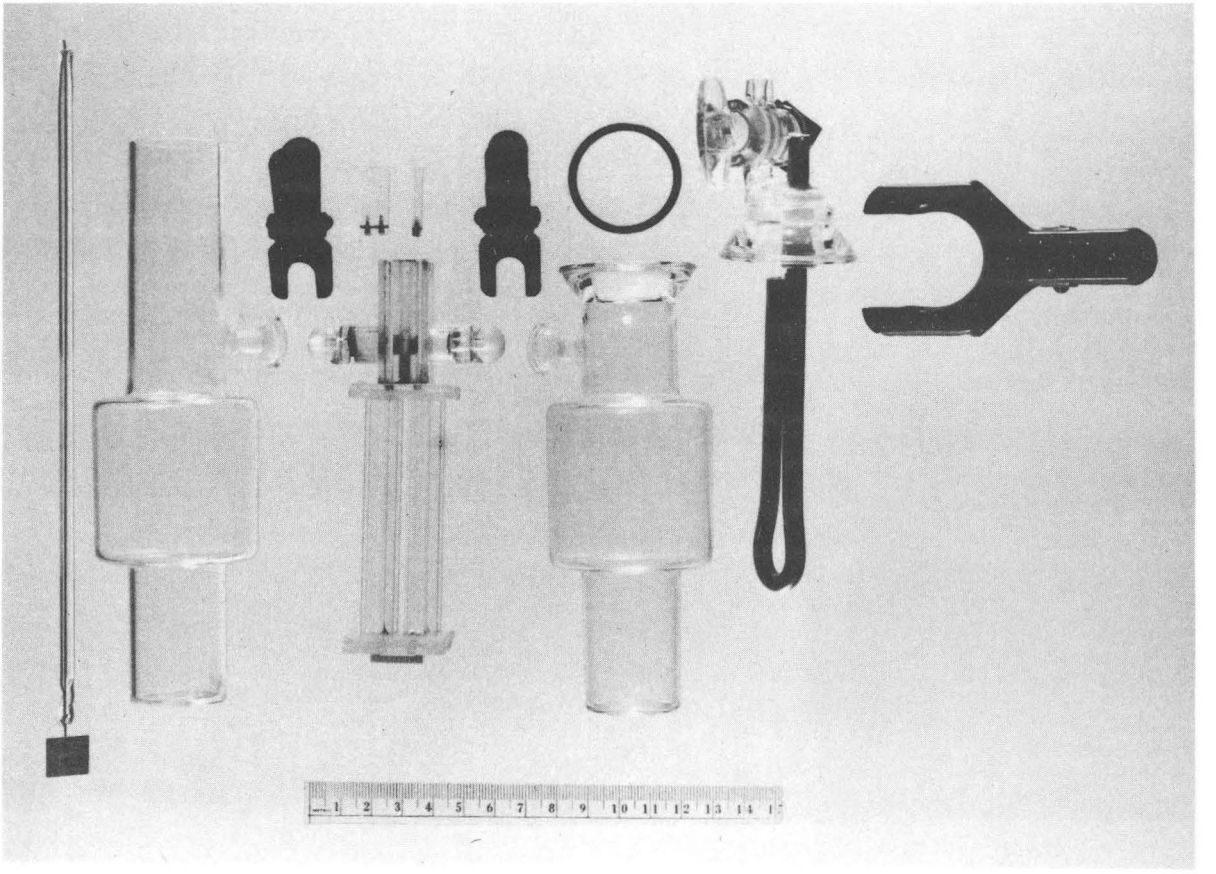

XBB 679-5170

Fig. 5. Blowup of Tiselius cell. (Reproduced from Milios' thesis for illustrative purposes.)

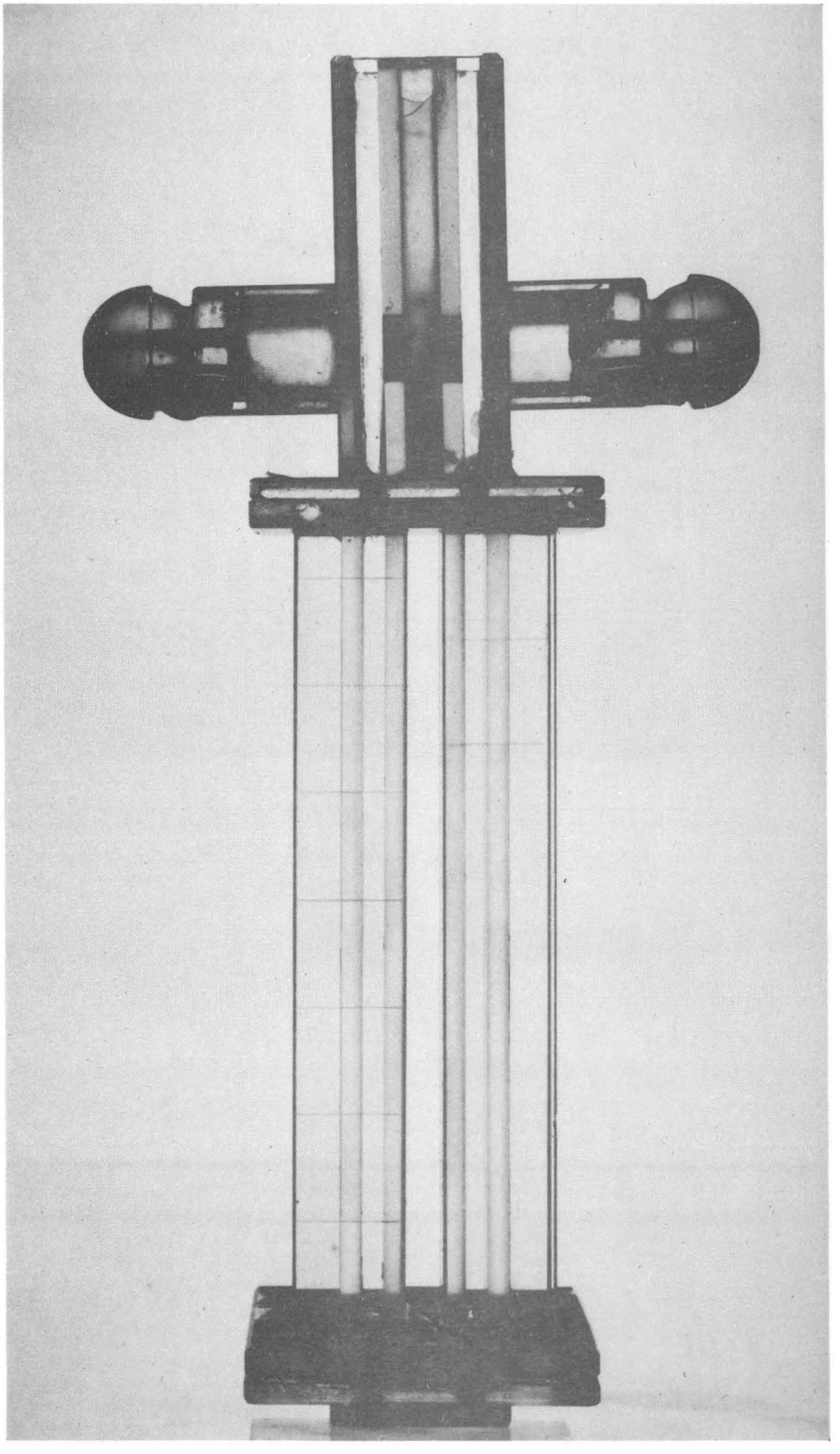

XBB 679-5168

Fig. 6. Close-up of Tiselius cell without electrode chambers. (Reproduced from Milios' thesis for illustrative purposes.)

The values $M_e = 107.880$ gm/gm mole

$\rho_e = 10.492$ gm/cm^3

and $F = 96{,}493$ coul/gm equivalent

are used.

III. 2. Calculation of $c_3/c_o|_{x = -\infty}$

A sizeable amount of reagent-grade ammonium nitrate bought from Merck & Co., Inc., Rahway, N. J., was stored in a vacuum oven purchased from the Precision Scientific Co., Chicago, Illinois (serial no. 19-G-12). It was estimated that the mean temperature over the solid was 90°C. A value for the concentration was chosen, with the weight of distilled water usually put at 1000 gm, and an approximate weight of the salt was calculated. The appropriate glassware, meanwhile, was being dried in another oven manufactured by the National Appliance Co., Portland, Oregon, at 70-80°C after having been soaked in warm (50-60°C) chromic acid cleaning solution (prepared in bulk) and rinsed thoroughly with distilled water.

To prepare the solution, both ovens were cooled to room temperature. The vacuum oven was brought to room pressure by bleeding air into it through a tube containing Drierite ($CaSO_4$). The salt and the weighing bottle(s) were then quickly transferred to a desiccator and taken to a Mettler balance. A slightly larger amount of salt (than that calculated) was weighted into the bottle(s). The bottle(s) and contents were returned to the vacuum-oven in the same desiccator and heated at 90°C under vacuum overnight (sometimes longer). The bottle(s) and contents were then transferred by the same means to the balances and weighed. After

transferring the salt to a 1000 ml flat-bottomed flask (which had been cleaned, dried and well stoppered) and stoppering it, the bottle and its remaining contents were weighed again. Care was taken during the weighing to note the deviations from the zero point of the Mettler balance and to correct for them as much as possible. The difference in the weighings gave the weight of dry salt in the flask. Weighed portions of distilled water were subsequently added to the salt in the flask. Thus the concentrations of the leading solution was shown, that is,

$$\left.\frac{c_3}{c_o}\right|_{x = -\infty} = \frac{\text{weight of salt}}{\text{M.W. of salt}} \times \frac{\text{M.W. of water}}{\text{wt. of water}} \tag{31}$$

The literature[13] equation for the density of NH_4NO_3 at 25°C,

$$\rho = 0.997077 + 0.032628\ c - 9.63 \times 10^{-4}\ c^{3/2} - 4.73 \times 10^{-5} c^2$$

$$[=]\text{gm/ml} \tag{32}$$

and the exact equation

$$\rho = \frac{1}{1000}\ (M_o c_o + Mc)\ \text{gm/ml} \tag{33}$$

together yield the two separate concentrations and subsequently the density of the solution present.

Table 1 lists the pertinent data.

Table 1. NH_4NO_3 solution data.

Run	Wt. NH_4NO_3 gm.	Wt. H_2O gm.	$c_3/c_o\|_{x=-\infty}$	$c_3\|_{x=-\infty}$ mole/liter	$c_o\|_{x=-\infty}$ mole/liter	ρ gm/ml.
A21,22	89.4414	1017.7070	1.97799×10^{-2}	1.039406	52.5487	1.02992
A31,32	1.1279	1120.0741	2.26637×10^{-4}	0.0125355	55.3109	0.99748
A41,42	35.5139	867.8858	9.20966×10^{-3}	0.497462	54.0152	1.01296
A51,52	6.5586	822.0403	1.79567×10^{-3}	0.098909	55.0820	1.00027

As for the concentration of the following solution, there were several points involved about it.

(a) Its density should be higher than that of the leading solution for a rising boundary to be realized.

(b) At the same time, its density should not be so close to that of the leading solution that it finds itself beneath its denser, adjusted counterpart (as a result of the Kohlrausch regulating function).

(c) Also, its density should not be so different from that of the leading solution that the concentration boundary set up between the adjusted and the initial solution could not be detected distinctly by the Rayleigh optics within a reasonable period of time.

(d) Finally, its concentration should be such that the ϵ_2 as a result of the concentration boundary between it and the adjusted concentration is at a minimum.

A mild stroke of luck with the first set of solutions pointed out a rough guide, namely,

$$\frac{c_3|_{x=-\infty}}{c_{initial}} = 1.02 \qquad (34)$$

that proved to be a profitable investment.

With the above in mind, then, after the concentration of the leading solution became evident, an approximate value for the initial concentration of the following solution was obtained.

Again, appealing to the literature equation[13] for the density of silver nitrate at 25°C and the exact expression for it,

$$\rho = 0.997074 + 0.141956c - 0.002603c^{3/2} = \frac{1}{1000}(M_o c_o + Mc) \qquad (35)$$

the ratio $c_{initial}/c_{oi}|_{x=+\infty}$ was obtained, leading therefore to a value for the weight of salt required.

The ratio of the weight of salt to that of water was zealously adhered to in the subsequent preparation of the following solution. In general, the procedures involved were similar to those mentioned earlier. A vacuum oven was not used, however, as $AgNO_3$ is not hygroscopic in nature. The salt was generally weighed in by the difference technique, and any difference between it and the calculated weight was compensated for by the weight of water subsequently added to the container.

The relevant data are quoted in Table 2.

Table 2. Concentration and density data of the set of following solutions.

Run	Wt. $AgNO_3$ gm	Wt. H_2O gm	$c_{initial}$ / $c_{o\ initial}$ at $x=+\infty$	$c_{initial}$ at $x=+\infty$ mole/liter	$c_{oi}\|_{x=+\infty}$ mole/liter	$\rho_{initial}$ gm/ml
A21,A22	174.6771	976.6443	1.89669×10^{-2}	1.016982	53.6189	1.13877
A31,A32	2.0786	992.0731	2.22189×10^{-4}	0.0122925	55.3246	0.99882
A41,A42	85.2681	1013.3095	8.92360×10^{-3}	0.486695	54.5402	1.06528
A51,A52	13.4899	817.6337	1.74963×10^{-3}	0.096562	55.1898	1.01070

III. 3. Determination of V

(a) Base Volume Calibration. The Milios cell-center unfortunately suffered an irreparable mishap at an early stage in the experiment. Consequently no attention was paid to his calibration data. Instead, another 9 mm interference cell-center previously used by Chapman in his diffusion measurements[11] (bearing his 2 reference lines on one optical face of the cell piece) was employed. Six lines were scribed onto the same face by the Precision Shop of the Lawrence Radiation Laboratory, with one of the Chapman lines as the baseline, and at a distance of 1 cm from one another. As the other Chapman line was not at a whole number of centimeters away from the base line, it found itself between two newly scribed marks. As a result there are eight lines on that face. The distances between those lines were carefully measured by the personnel in the Precision Shop with a platform microscope. The measurements were done along the channel on the optical face, and within this small space three sets of distances were obtained, one on the left of the space, one along the middle, and one on the right. The data are listed in Table 3.

Table 3. Data on lengths between reference lines on one optical face of the Tiselius cell.

Line numbers are as indicated.

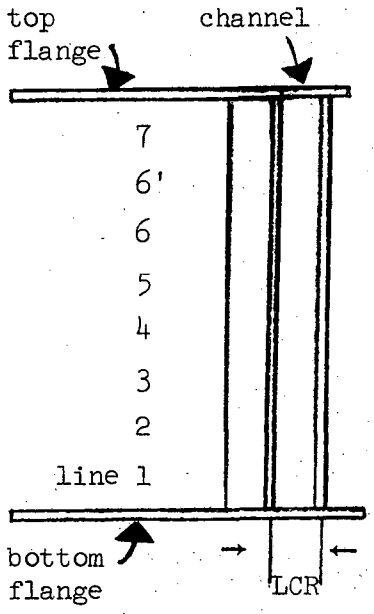

Length measured	Data in inches (7/9/69) (left) L	(center) C	(right) R	Average in inches	Average in centimeters
1-2	0.3934	0.3936	0.3934	0.3935	0.9995
2-3	0.3918	0.3916	0.3919	0.3918	0.9952
3-4	0.3942	0.3942	0.3941	0.3942	1.0013
4-5	0.3934	0.3934	0.3934	0.3934	0.9992
5-6	0.3913	0.3917	0.3919	0.3916	0.9947
(6-6'	0.1034	0.1030	0.1026	0.1030	0.2616)
6-7	0.3941	0.3936	0.3935	0.3937	1.0000
					Σ = 5.9899
Overall length 1-7	2.3582	2.3581	2.3582	2.3582	5.9898

As it was Milios' experience that the cross-sectional area of his cell-center was not uniform (i.e., not exactly 9 mm X 2 mm as reported by Perkin-Elmer), it was decided that a mercury calibration done on the Chapman cell-piece was necessary in order that a more complete documentation of the piece's cross-sectional area along its length would be available for subsequent analysis. The calibration was done for every centimeter of cell-length; the procedure adopted is as follows,

(i) the bottom of the cell-center, i.e., the end with the Chapman base-line closest to it, was closed off with a piece of ground-glass of similar shape and size to a cell-flange (Apiezon N vacuum grease made by British Shell was the sealant used). Rubber bands were stretched into service around the flange and ground-glass to ensure a tight seal.

(ii) Clean mercury (Ballard's triple-distilled version, from Quicksilver Products, Inc., San Francisco, California) was carefully weighed out and transferred to the channel until the newly-formed meniscus just reached (according to squinty eye-balling) the first cell-mark or the Chapman base-line. As the cell-center without the electrode chambers and holder could be supported in the bath of the electrophoresis apparatus by carefully sliding the top flange over the narrow top of the flat mirror at the rear of the bath, this procedure was readily pressed into service. The water-level in the bath (held at 25°C) was adjusted so that it did not quite reach the top of the flat mirror; otherwise, it was discovered, the cell flange on top of the mirror would slip over the film of water between it and the mirror, and the circulation in the bath proper sooner or later would cause the whole contraption to fall into

the water (an entirely undesirable situation). It was also noticed that the cell tended to slant down toward the water, due in large part to the difference in horizontal orientation between its flange and the mirror top.

The mercury was allowed to reach thermal equilibrium. Meanwhile, the Rayleigh optical system was activated in the apparatus, and the orientation of the flat mirror was slightly adjusted so that a picture taken of the cell-center (with its lined face adjacent to the mirror) would show all eight lines clearly. A picture was then taken of the cell in order that a decision could be formulated as to whether the meniscus was at the position desired, i.e., at the first cell-mark. If not (as was generally the case), the cell-center was removed, and more (or less) mercury was weighed into it (or out of it). It was again placed into the bath, and after equilibrium was reached (during which time weighings were accomplished) another picture was taken. This procedure was repeated (in general, the second or third try would net the desired result) until it was felt that the meniscus was indeed at the right position immediately touching a reference mark. Although human error in judgment was undoubtedly present, it was felt that the consistency in the placement of menisci near the marks would largely compensate for it. The prior and posterior weights of the glass vessel (not the cell-center) containing the mercury gave the weight of the mercury inside the optical cell-piece.

The sequence was repeated for the line immediately above the base-line, and another weight of mercury was obtained. This weight, when

divided by the density of mercury at 25°C, 13.5336 gm/cc (from Perry's Handbook[14]) gave the volume of Hg between the two menisci. It was then assumed that the shape of the menisci remained the same for both pictures. The distance between lines 1, the base-line, and 2, from the Precision Shop measurements, was then used to compute the average cross-sectional area between these two lines.

The same procedure was performed for the other pairings. The results are shown in Table 4.

The overall volume between lines 1 and 7 is the product of the average length 5.9898 cm and the average cross-sectional area, 0.17967 cm^2 and is 1.0762 cm^3.

Table 4. Base volume data (see sketch in Table 3 for positions of line numbers 1-7) 1 is bottommost line, 7 is topmost.

	Distance between reference lines, cm (taken to be height of mercury column)(from Table 3)	Weight of mercury, gm within specified length	Density of mercury at 25°C gm/cm^3	Volume of mercury, cm^3 within specified length	Cross-sectional area in channel, averaged over specified length of cell, cm^2
1-2	0.9995	2.4368	13.5336	0.18006	0.18015
2-3	0.9952	2.4211	13.5336	0.17890	0.17976
3-4	1.0013	2.4420	13.5336	0.18044	0.18021
4-5	0.9992	2.4317	13.5336	0.17968	0.17982
5-6	0.9947	2.4274	13.5336	0.17936	0.18032
6-7	1.0000	2.4053	13.5336	0.17773	0.17773
				Average:	0.17967 ± 0.00100 cm^2

$$V_{1-7} = L_{1-7} X \text{ (average cross-sectional area of channel)}$$

$$= 5.9898 \ (0.17967) \text{ cm}^3$$

$$= 1.07619 \text{ cm}^3 \text{ or } 1.0762 \text{ cm}^3$$

(b) Volume covered by the moving boundary

This section will be subdivided into the following parts.

(i) Cell-filling

(ii) Boundary observation

(iii) Volume analysis

(For a description of the optical cell and cell-holder see Chapman,[11] p. 116)

(i) The cell top supplied by Perkin-Elmer was modified to include ball-joints at the two side-arm positions and a permanently glued-in cell-gate to block off the openings opposite the two side-arms so that solution could not leak from one channel to the other. The epoxy glue used was a 50-50 mixture of "Epon" 820 and "Versamide" 140 supplied by the Plastics Shop of the Lawrence Radiation Laboratory.

The assembly of cell parts was usually soaked for 2-3 minutes in warm chromic acid solution, rinsed thoroughly with distilled water, and oven-dried until a run was to be made. They were then removed with Kim-wipes (Kimberly-Clark Corp., Neenan, Wisconsin) and assembled with Apiezon N grease (a Royal Shell product supplied in the USA by James G. Biddle Co., Plymouth Meeting, Pa.). The procedure was first to assemble the center and bottom pieces. In general, a thin film of grease was smeared onto a flange of one of the pieces and applied evenly over the area with a Puritan wooden applicator (Hardwood Products Co., Guilford, Maine). Areas about a millimeter or two wide around the perimeters of the channel openings were left bare to avoid getting excess grease into the channels. The other cell piece was then attached to it, with mild pressure being applied to the adjacent flanges. The pieces were rotated slightly in

opposite directions. They were also made to slide upon each other until the whole area between flanges became transparent. The cell-top was added onto this partial assembly in the same manner. Any grease accidentally smeared onto the exterior of the sections was removed by wiping the contaminated area with Kodak Lens Cleaning Paper (Eastman Kodak Co., Rochester, N. Y.) .

A cell-holder supplied by Perkin-Elmer held the cell in place. This particular holder had been previously modified by Chapman (see his thesis,[11] for discussion and details) in order that the cell could be held in place in a balanced manner tension-wise. The cell is held by being clamped from the outside flanges; that is, it rests on the bottom one while spring tension is applied on the top. Mechanical linkages in the cell-holder allow both the top and bottom sections to be displaced from the center by manipulation of the two knobs at the top in the directions indicated. This allows the center section, which is stationary, to be closed off at the outer surfaces of its flanges by the opposing flange surfaces.

The face of the cell on which the reference lines were scribed was oriented in the holder such that it was close to the flat mirror at the rear of the bath.

To fill the cell all channels were aligned by manipulating the two top knobs appropriately. A 10 cc glass-tipped syringe with a 7-inch 18-gauge hypodermic needle (90% platinum, 10% ruthenium, supplied by the Hamilton Co., Inc., Whittier, California) was used to transfer $AgNO_3$ solution from and to a small glass container (the 1000 cc flask was shaken violently and repeatedly just before solution was transferred to the

container). With the cell tilted toward the side of the unmarked channel for air to escape, the needle was inserted carefully into the channel all the way to the bottom, and solution was slowly forced from it until the space in the bottom section (the U-shaped space) was full of it and a short length of solution was in each leg of the center piece. The needle was withdrawn, and the holder put back on its supports. Care was taken when withdrawing the needle to avoid letting it pick up any grease from the flange joints and smearing it onto the interior of the channel. The bottom space was examined for bubbles. If some were present in the longitudinal direction of the channel, the needle was inserted to dislodge them. If they were lodged somewhere in the center of the space, the solution was withdrawn completely (with the holder again in a tilted position) and the filling procedure repeated again. The bottom section was then displaced from the aligned position by turning the knob controlling it in the appropriate direction.

The small amount of $AgNO_3$ in the marked channel was removed with the same syringe assembly. The unmarked channel was then filled with more $AgNO_3$ solution until its entire length up to the sidearm outlets was filled (the same syringe needle was used). Another similar syringe assembly was used to rinse the marked channel with NH_4NO_3 solution at least five times, care being taken every time to avoid contaminating the parent volume of NH_4NO_3 with the rinsing portion. The marked channel was then filled with ammonium nitrate solution up to the sidearm outlet. The two channels were carefully examined for bubbles, and those present were removed immediately.

The cathode chamber (a modified Perkin-Elmer buffer bottle with a higher top) with ammonium nitrate solution up to its sidearm was attached with Apiezon grease to the ball-joint leading away from the sidearm on the side of the marked channel. The attachment was further tightened and strengthened with a small clamp. The syringe assembly for ammonium nitrate was used to transfer more liquid slowly to the chamber until the channel in the cell-top was filled completely. A lucite plug with a slightly enlarged rubber band around its lower end, having been smeared all over with Apiezon N grease, was inserted into the channel opening (the plug, of a similar size and shape to the channel opening, was manufactured by the Machine Shop of the Inorganic Materials Research Division of the Radiation Laboratory), thus displacing the liquid originally there to the chamber side. The rectangular loop around the plug outside the opening was loaded with a thick layer of grease to discourage leakage therefrom. The cathode, a small, squarish piece of stainless steel at one tip of a thin tungsten rod vacuum-sealed in a uranium glass envelope, having been rinsed with ammonium nitrate solution earlier, was placed in the chamber. The stainless steel plate had been wiped clean a little while earlier.

As for the anode side, the chamber with silver nitrate was attached to the cell and the assembly filled with solution in the same manner. Before the channel top was filled completely, however, due to the particular arrangement of the anode in the chamber-top, the chamber-top with the silver rod was attached to the chamber bottle. An appropriate "O" rubber ring, which fitted into the groove, served to seal tightly the two factions together. Apiezon grease was used around the "O"

ring and along the grooves. With the stopcock opened to the atmosphere, the silver nitrate needle assembly was inserted through the stopcock pore into the chamber, and the channel top filled completely. Another lucite plug, of similar structure to the one mentioned earlier, was inserted with the aid of a generous dose of Apiezon grease. The anode chamber was then filled with solution until the liquid level went past the upper mouth of the pore opening in the stopcock and into the short tubing facing the air. The stopcock was closed.

It should be kept in mind that the lucite plugs were inserted into the channels in such a manner that no bubbles were trapped beneath them.

The whole system, after being treated to a final visual check for bubbles, was placed in the bath, guided by the two posts in it. There was an even circulation of the bath water as a result of the centrifugal pump (an integral part of the apparatus) being in action. A Sargent Thermonitor (manufactured by E. H. Sargent & Co., Chicago, Illinois) maintained the water temperature at 25°C.

With the cell assembly in the bath, the mercury lamp was activated, and the appropriate panel knobs on the electrophoresis apparatus were adjusted until an image of the cell-center was visible on the viewing screen. As bubbles frequently lodged themselves beneath the flanges between the top and center sections of the cell when the whole assembly was immersed into the water, they revealed themselves very vividly as dark dots against the green background on the screen. They were readily removed by lifting the holder by its handle up past the area with bubbles from the water and then re-immersing it repeatedly until the dark dots disappeared. The assembly was then slid toward the flat mirror and

into position. Thermal equilibrium was assumed to be reached when thirty minutes or more had elapsed.

On several occasions, it was discovered that the liquid level in the anode chamber sank a little while the whole assembly was striving toward temperature equilibrium. Apparently, air spaces had not been completely replaced by solution during filling procedures around and inside the short length of glass-casing that served to hold the silver rod in place at the chamber-top. This situation was readily corrected by inserting more $AgNO_3$ solution into the chamber with the same silver nitrate needle assembly. (Efforts were made after these particular runs with the phenomenon just mentioned to improve on the sealing in and around the casing to minimize the possibility of air-spaces.) The silver anode was rinsed with the silver nitrate solution used during the run before it was inserted into the chamber bottle. The ball-joint at the sidearm on the following solution side, and the joint between the anode chamber top and the chamber proper, were securely tightened with proper-sized clamps.

(ii) With the electrical arrangement at the ready, leakage tests were performed (see Section III.5 for details) between (a) the cathode and the anode, (b) the cathode and a bath electrode situated at one corner of the bath away from the flat mirror, and (c) the anode and the bath electrode. The resulting currents were deemed negligible if they were in the order of 1 microAmpere or less. Test (a) in all the runs produced satisfactory results, while the other two sometimes indicated that minor leakages were present. As far as the anode was concerned, these leakages were easily corrected for by re-sealing the appropriate

contact areas around the rod at the chamber-top, and in and around the glass-tube casing enveloping the rod immediately below the chamber-top, with the Dow-Corning adhesive sealant. As for the cathode leakages, it was found that a replacement of chamber bottles had to be administered in order to bring about a lessening of them to negligible levels.

With the electrical system again at the ready, the bottom section of the optical cell was aligned, after all three successful passes leakage-wise had been achieved. The two-salt boundary that was immediately formed was allowed to stabilize for five to ten minutes. With the set current on, the boundary movement was traced with the Rayleigh optics available; the green mercury light offered a clear image of the boundary on the viewing screen. The combination Schlieren derivative curve-Rayleigh fringes arrangement offered an excellent tracing mechanism, in the sense that the sharp fringes and the dark Schlieren lateral peak against the green background were very visible on the screen. The angle of the analyzer diaphragm was monitored in order that the clearest boundary outline (i.e., the derivative curve or peak) was available for photography.

When the boundary reached a space between two reference lines, the mercury lamp was de-activated and the tungsten source switched on. (This between-lines arrangement was preferred to that with the boundary astriding one line, i.e., with the boundary being dissected about equally by the line, for the sake of the microphotometer analysis of the negatives later on.) With the optics set for picture-taking as directed by the apparatus manual, the shutter provided was opened, the timer system set, and the shutter was then closed. It was judged that about equal times

elapsed between the opening of the shutter and the timer action, and between the latter and the closing. The exposure time, in the order of two to four seconds, introduced some uncertainty in the time variable as it could not in reality be reproduced. An MP-3 Type Industrial View Land Camera back, projection film Type 46L (800 speed transparency film, 3 1/4" x 4"), and Dippit Solution #646, supplied by the Polaroid Corp., Cambridge, Massachusetts, together constituted the exterior photography arrangement.

The exposed negative was allowed to develop for at least three minutes inside the camera back. It was then subjected to vigorous contact through shaking upright with the Dippit solution for twenty seconds, after which it was air-dried. The appropriate film number and other identification numbers were taped onto it. When it struck this experimenter's fancy, negatives were also taken of the combination curve-fringe phenomenon, as its visual quality was felt to be quite satisfying as well as educational. They were not used, however, in the later microphotometer analysis.

The boundary motion was usually captured on film at five or more locations in order that sufficient data could be generated for a complete monitoring of the boundary velocity to be realized. This precautionary step was taken to provide for a reliable criterion, which was later used in the company of others to ascertain the quality of the run just completed.

(iii) The set of Schlieren pictures was analyzed with a Jarrell-Ash Microphotometer located in the Technical Photography section of the Inorganic Materials Research Division. The analysis was composed of the

following steps. The transparency was placed on the travelling stage of the instrument with a piece of optical-quality glass plate on top of it to hold it flat. The stage was manually rotated until the reference lines bordering the boundary peak were perpendicular to its direction of longitudinal travel. With the slit dimensions set (the photoelectric cell behind the slit supplies a signal which is plotted on a chart recorder) the transparency was given a quick scanning at a previously decided location (i.e., a line which would dissect the peak at a certain fraction of its height) in the region with the peak so that the sensitivity device in the instrument could be set to yield the desired low and high transmittances within a relative scale of 0-100% on the recording chart. The low setting, of course, corresponded to the reference lines, and the high could usually be located in areas immediately adjacent to the curve as they were the brightest. With everything set, the automatic longitudinal motor-drive was activated at a set, constant velocity, and the region with the peak was scanned twice. The intensity peaks so recorded as a result of the two reference lines being present allowed absolute distances to be measured. The boundary was recorded as two smaller (as the derivative curve was not as intense as the reference lines) peaks close together, with their center taken as its absolute location. The two measurements for each transparency produced an averaged ratio of the distance between the boundary and the line nearer to it and that between the two reference lines. The absolute version of the former was obtained later by comparing the ratio with the real distance measured by the Precision Shop (cf. Table 3). The other transparencies for the same run were similarly treated,

with the same fraction of the peak traversed over the photoelectric cell slit in every case. The resulting locations of the boundary, and the corresponding time-intervals between them, were used for the velocity and volume calculations.

Table 5, listing velocity data for two runs, offers an insight into the technique of monitoring runs. The method with which time-intervals between negatives were recorded is discussed in the next section.

The results of the volume calculations are presented in Table 6. It is apparent from it that for every experimental run performed, at least two sets of moving boundary data were collected, with the first negative depicting the boundary near the base reference line taken as the common index for the other negatives obtained near the end of the run. This arrangement was preferred to that involving the taking of two or more distinct sets of negatives for expediency's sake as far as the time measurement scheme was concerned. The volumes computed enter accordingly (as V's) into the transference number equation, Eq. (30).

Table 5. An example of two runs being monitored.

Run	Film #	Boundary location cm	Time recorded between films sec	Distance traveled cm	Velocity cm/sec
A21	1	ℓ1B=0.0341			
			1,744.41	0.9854	0.000565
	2	ℓ2B=0.0200			
			1,848.09	1.0466	0.000566
	3	ℓ3B=0.0714			
			2,056.12	1.1602	0.000564
	4	ℓ4B=0.2303			
			1,420.00	0.8096	0.000570
	5	ℓ5B=0.0407			
			847.74	0.4831	0.000570
	6	Bℓ6=0.4709			
			828.87	0.4795	0.000579
	7	ℓ6B=0.0086			
			553.20	0.3201	0.000579
	8	ℓ6'B=0.0585			
A22	1	Bℓ2=0.3898			
			3,103.19	0.8969	0.000289
	2	Bℓ3=0.4881			
			4,440.17	1.2580	0.000283
	3	Bℓ4=0.2314			
			2,886.97	0.8322	0.000288
	4	Bℓ5=0.3984			
			2,739.01	0.7848	0.000287
	5	ℓ5B=0.3864			
			1,230.40	0.3560	0.000289
	6	Bℓ6=0.2523			
			1,237.82	0.3575	0.000289
	7	ℓ6B=0.1052			

"Bℓ2" = distance between boundary and reference line 2

"ℓ2B" = distance between reference line 2 and boundary

For order in which reference lines are numbered, see Table 3

Table 6. Volume covered by moving boundary.

Run		$V_{1:7}$ cm^3 (from table 4)	Film #	Boundary location 1, cm (near bottom line)	$-\Delta V_1$ cm^3	Film #	Boundary location 2, cm (near top line)	$-\Delta V_2$ cm^3	$V=V_{1:7}-(\Delta V_1+\Delta V_2)$ cm^3
A21	a	1.0762	1	ℓ1B=0.0341	0.0061	6	Bℓ6=0.4709	0.2643	0.8058
	b	1.0762	1	ℓ1B=0.0341	0.0061	7	ℓ6B=0.0086	0.1781	0.8920
	c	1.0762	1	ℓ1B=0.0341	0.0061	8	ℓ6'B=0.0585	0.1222	0.9479
A22	a	1.0762	1	Bℓ2=0.3898	0.1095	6	Bℓ6=0.2523	0.2250	0.7417
	b	1.0762	1	Bℓ2=0.3898	0.1095	7	ℓ6B=0.1052	0.1608	0.8059
A31	a	1.0762	1	Bℓ2=0.4972	0.0902	4	ℓ5B=0.2934	0.3057	0.6803
	b	1.0762	1	Bℓ2=0.4972	0.0902	5	Bℓ6=0.3725	0.2466	0.7394
A32	a	1.0762	1	Bℓ2=0.4239	0.1034	3	ℓ5B=0.2343	0.3163	0.6565
	b	1.0762	1	Bℓ2=0.4239	0.1034	4	Bℓ6=0.3317	0.2393	0.7335
A41	a	1.0762	1	Bℓ2=0.4170	0.1721	3	ℓ5B=0.1306	0.3349	0.5692
	b	1.0762	1	Bℓ2=0.4170	0.1721	4	Bℓ6=0.4451	0.2596	0.6445
A42	a	1.0762	1	ℓ2B=0.0623	0.1908	4	ℓ5B=0.0324	0.3526	0.5328
	b	1.0762	1	ℓ2B=0.0623	0.1908	5	Bℓ6=0.3356	0.2400	0.6454
A51	a	1.0762	1	ℓ2B=0.4290	0.2567	3	Bℓ5=0.0051	0.3593	0.4602
	b	1.0762	1	ℓ2B=0.4290	0.2567	4	Bℓ6=0.4403	0.2588	0.5607
	c	1.0762	1	ℓ2B=0.4290	0.2567	5	ℓ6B=0.0203	0.1760	0.6435
A52	a	1.0762	1	Bℓ2=0.4348	0.1015	5	ℓ5B=0.2381	0.3156	0.6591
	b	1.0762	1	Bℓ2=0.4348	0.1015	6	ℓ6B=0.0312	0.1741	0.8006
	c	1.0762	1	Bℓ2=0.4348	0.1015	7	ℓ6B=0.3203	0.1221	0.8526

"Bℓ2" = distance between boundary & reference line 2

"ℓ2B"=distance between reference line 2 & boundary

For order in which reference lines are numbered see Table 3

III. 4. The Recording of the Time-Variable, t

The set of timing devices used included the following,

(i) two electric timers, catalog no. 69235, made by the Precision Scientific Co. Chicago, Illinois (labelled Timer A and B for easy identification), and

(ii) three Swiss-made antimagnetic stopwatches, distributed in the United States by the West Coast Swiss Watch Co., San Francisco, California.

At the moment the first negative was being exposed to the phenomenon in the bath, the two timers and two of the watches (clearly numbered) were activated. One of the latter was stopped and the heretofore inactive third stopwatch pressed on at the moment the second negative was taken. These two stopwatches then traced out a cascade of time-intervals for the intermediate transparencies. The negatives with the combination fringe-curve pattern were not time-traced. When it came time for the first of the decisive volume negatives to be exposed, the stopwatch in the sequence still running and the one activated at the very beginning were simultaneously switched off. When it came time for the second negative to be exposed, one of the timers was de-activated. The other timer then recorded the corresponding time-interval for the third volume transparency.

When only two sets of data were desired, i.e., when dealing with solutions that were on the dilute side, the two timers and two stopwatches were used.

As a precautionary measure, the two types of time pieces were made to run against one another several times, and any discrepancies in the

times recorded were noted and subsequently taken into account in the final calculations. Evidently, the two electric timers were considered the more reliable among the time-pieces.

The adjusted run times are listed in Table 7.

Table 7. The adjusted times for the runs (in seconds).

Run	t
A_{21}	7,916.34
	8,745.18
	9,298.38
A_{22}	14,399.28
	15,636.78
A_{31}	3,274.98
	3,566.76
A_{32}	2,129.28
	2,375.88
A_{41}	5,299.56
	6,001.56
A_{42}	3,358.80
	4,057.68
A_{51}	1,728.18
	2,104.26
	2,420.71
A_{52}	1,645.32
	1,997.28
	2,140.54

III. 5. The Recording of the Time-averaged Current, I

The equipment central to this aspect of the present work involved the following,

(a) a Regatron constant-currect power supply, model 612A, from Electronic Measurements, a division of the Rowan Controller Co., Eatontown, New Jersey,

(b) a standard four-terminal resistor, cat. no. 4030-B, from the Leeds and Northrup Co., North Wales, Pennsylvania,with a two-terminal value at 25°C of 99.9999 ohms,

(c) a potentiometric strip chart recorder, model SRG, cat. no. S72180-15, from E. H. Sargent & Co., Chicago, Illinois,

(d) a differential voltmeter, model 3420A, from the Hewlett & Packard Co., Palo Alto, California,

and (e) a compensating polar planimeter, no. 620005, from the Keuffel & Esser Co., New York, New York.

Component (a), of course, supplied the particular current for each run. Component (b), with its two side-thumb screw terminals placed in series with the power-source-cell electrodes arrangement, could be (and was) linked also with the differential voltmeter through its two top thumbscrews. The hole in the head of the resistor case provided a convenient site for the insertion of a suitable thermometer to provide for temperature monitoring during runs. The voltmeter output was continuously traced on the Sargent chart-recorder. Component (e) was employed to measure traced-out areas on the recorder.

As stabilization of the current output was very much desired, the power source was activated several hours before a run was made, with the

cell-electrodes bypassed. The process of stabilization involved also a prior setting of the amplitude of the voltmeter output and the pen span on the chart recorder. In this way, with the pen zeroed in the center of the chart, the recorder output could be calibrated by means of unit variations in either direction in the voltmeter setting, with the range set in such a manner that later analysis of the traced area was facilitated. In practice, the recorder output was allowed to run at the lowest chart speed of 0.2 in./min for an appreciably long period of time (about two to three hours) before the actual voltage-area traced calibrations were performed. The amplifier gain control on the Sargent recorder was adjusted during the early portion of the stabilization process to a point such that an optimal balance without oscillations in the pen motion was achieved.

With the cell assembly properly set in the bath, leakage checks of the nature mentioned earlier were performed. The recorder input was discontinued, and with the bottom section of the Tiselius cell displaced from its aligned position each of the three electrode pairings was checked by placing it in series with the power source. The voltmeter readings obtained by the passage of the set amount of current through the pairings then yielded the leaked current data necessary for a decision to be made as to whether to proceed with the run or not. As pointed out earlier, amounts in the order of one microAmpere were deemed satisfactory.

As soon as enough stabilization was achieved, the voltmeter setting corresponding to a zeroing of the chart pen was noted. The resistor

temperature was then recorded. Finally, after the two-salt boundary had sufficiently stabilized itself, i.e., when five to ten minutes had elapsed after the aligning of the bottom section, the cell was placed in series with the power source. The recorder in all instances ran at the slowest speed of 0.2 in./min. Variations in the resistor and bath temperatures were recorded during the runs.

As soon as the last of the volume negatives was taken, the cell was taken out of series with the current circuit, and the concentration boundary within the body of the following solution was searched for (see the next section for details). When this task was completed, the same series of leakage tests were done as a final check on the run as a whole. It was found that in all cases in which the first series yielded go-ahead results the second set only served to reinforce the validity of what had gone on before.

The recorder output generated for each run was analyzed with the polar planimeter cited earlier. With the calibrated voltage values and the time-intervals recorded, the current drifts from its set value were time-averaged. As the resistor usually ran at temperatures slightly higher than room temperature, its two-terminal value was adjusted for the temperature difference present in each case, using the temperature-coefficient constants given in the manual. It turned out to be either 100.0006 or 100.0007 ohms in all the runs. The time-averaged drifts were taken into account in the final report of the adjusted current, I, in milliAmperes, listed in Table 8.

Table 8. The adjusted current I, in milliamps.

Run	E_o volt(s)	ΔE volt(s)	E volt(s)	Ω	I
A21	2.00622	-0.000021	2.006241	100.0007	20.06227
	2.00622	-0.000004	2.006216	100.0007	20.06202
	2.00622	-0.000024	2.006196	100.0007	20.06182
A22	1.01000	-0.000413	1.009587	100.0007	10.09580
	1.01000	-0.000415	1.009585	100.0007	10.09578
A31	0.050566	-0.0000015	0.0505645	100.0006	0.50564
	0.050566	-0.0000016	0.0505644	100.0006	0.50564
A32	0.074945	+0.0000018	0.0749468	100.0006	0.74946
	0.074945	+0.0000017	0.0749467	100.0006	0.74946
A41	1.01575	+0.000102	1.015852	100.0006	10.15846
	1.01575	+0.000095	1.015845	100.0006	10.15839
A42	1.49970	+0.000064	1.499764	100.0006	14.99756
	1.49970	+0.000060	1.499760	100.0006	14.99752
A51	0.501100	+0.0000594	0.5011594	100.0007	5.01156
	0.501100	+0.0000644	0.5011644	100.0007	5.01161
	0.501100	+0.0000612	0.5011612	100.0007	5.01158
A52	0.751700	+0.000031	0.751731	100.0007	7.51726
	0.751700	+0.000029	0.751729	100.0007	7.51724
	0.751700	+0.000029	0.751729	100.0007	7.51724

III. 5. The parameters a_B and b_B

With the following values for the coefficients in the expressions for these two parameters at hand (see Milios,[1] p. 38),

$$e = k_1/M_o = 55.3438 \text{ moles/liter}; \; g = k_3/M_o = -0.1445 \; (\text{moles/l.})^{-1/2}$$

$$f = (k_2 - M)/M_o = -1.5504; \text{ and } h = k_4/M_o = 0.0 \quad ,$$

the concentration data quoted in Table 2 for the initially-prepared silver nitrate solutions were substituted into equations (26) and (27) (reproduced below for easy reference) to generate the information in Table 9.

$$a = e - \frac{1}{2} gc_i^{3/2}[1 + \frac{3}{4}\epsilon + \frac{1}{80}\epsilon^2 + O(\epsilon^3)] - hc_i^2(1 + \epsilon + \frac{1}{6}\epsilon^2) \qquad (26)$$

$$b = f + \frac{3}{2} gc_i^{1/2}[1 + \frac{1}{4}\epsilon + O(\epsilon^2)] + 2hc_i(1 + \frac{1}{2}\epsilon) \qquad (27)$$

Table 9. a_B and b_B

Runs	a_B	b_B
$A_{21,22}$	$55.3438 + 0.0741[1+(3/4)\epsilon+(1/80)\epsilon^2]$	$-1.5504 - 0.2186[1+(1/4)\epsilon]$
$A_{31,32}$	$55.3438 + 0.0001[1+(3/4)\epsilon+(1/80)\epsilon^2]$	$-1.5504 - 0.0240[1+(1/4)\epsilon]$
$A_{41,42}$	$55.3438 + 0.0245[1+(3/4)\epsilon+(1/80)\epsilon^2]$	$-1.5504 - 0.1512[1+(1/4)\epsilon]$
$A_{51,52}$	$55.3438 + 0.0022[1+(3/4)\epsilon+(1/80)\epsilon^2]$	$-1.5504 - 0.0674[1+(1/4)\epsilon]$

As the initially-prepared silver nitrate solutions were all more concentrated than those required by the Kohlrausch regulating function, ϵ in every case consisted of two contributions, ϵ_1 and ϵ_2 (see Section II.3).

ϵ_1 was estimated in the manner suggested by Milios. The method employed centered on one expression, namely,

$$\epsilon_1 \approx \frac{0.00932}{c}\left(\frac{I}{z_+ \nu_+ A_e}\right)^{0.8}\left(\frac{L}{\beta}\right)^{0.2} \tag{29}$$

where $c = c_{initial}$

$z_+, \nu_+ = 1$

$A_e = 5\ cm^2$ (effective value)

$L = 3$ cm (effective value)

and $\beta \approx (0.1419 - 0.0039\ c_i^{1/2})/\rho_B$

Table 10 lists the relevant data.

Table 10. Estimation of ϵ_1

Run	$c_i^{1/2}$ $(M)^{1/2}$	~I mA	ρ_B gm/ml	β liters/mole	ϵ_1
A_{21}	1.00846	20.0	1.1388	0.1213	0.05
A_{22}	1.00846	10.0	1.1388	0.1213	0.03
A_{31}	0.11087	0.5	0.9988	0.1418	0.22
A_{32}	0.11087	0.75	0.9988	0.1418	0.31
A_{41}	0.69764	10.0	1.0653	0.1308	0.06
A_{42}	0.69764	15.0	1.0653	0.1308	0.09
A_{51}	0.31074	5.0	1.0107	0.1393	0.17
A_{52}	0.31074	7.5	1.0107	0.1393	0.24

ϵ_2 was estimated using the Rayleigh interference optics in the following manner.

After the Schlieren run was completed, the cell assembly was gingerly removed from the bath so that the interference mask for the cell could be attached to its marked optical face. The assembly was re-immersed into the bath and any newly-formed bubbles (visible on the viewing screen as dark dots) were fastidiously removed. The short length of tubing protruding from the stopcock away from the anode top was then filled with the same silver nitrate solution that was in the anode chamber. The solution was then slowly and carefully drained into the chamber proper, care being taken to exclude the entrance of air. This procedure was performed several times until an accountable amount of liquid had been added to the assembly and the Rayleigh optics indicated that no more needed to be drained into it. The concentration boundary caused by the Kohlrausch function, in the form of a wavy fringe pattern when illuminated by the Rayleigh arrangement, was then at about the center of the cell-center on the viewing screen. Several transparencies were obtained of this phenomenon. The exposure times for them were on the order of twenty seconds, and as before, they were allowed to develop inside the camera back for at least three minutes, after which they were treated to a solidification process with the Dippit solution available. Identification marks were also taped onto them.

As for their analysis, the objective here was to estimate the concentration of the adjusted following solution immediately below the leading solution of NH_4NO_3. Since the initial concentration was known for all runs (cf. Table 2), the fringe shifts so recorded offered the concentration differential involved between it and the adjusted. The

proportionality constants needed to complete this estimation process were obtained by the following scheme.

Solutions of silver nitrate were carefully prepared (cf. Section III. 2) according to the criterion that the range of concentration covered by any pairing of solutions included the value of the concentration of the initially-prepared solution. Each pairing was then injected into a channel in the cell-center, with the heavier member at the bottom, and the lighter one added onto it with great care. As it was decided that a non-sharp boundary would not jeopardize the analysis to any great extent, the Motor-Driven Syringe Assembly available with the electrophoresis apparatus for sharp initial boundaries was not utilized. Instead, the pairings were allowed to diffuse into each other within the closed channels (glass-plates had been attached onto the top and bottom flanges of the cell-center with Apiezon grease), and the subsequent concentration boundaries formed were recorded on film as a function of diffusion time (to a maximum of two to three hours). Evidently, the cell-center was held in place in the holder, the whole assembly being controlled at 25°C in the bath. The fringe shifts so recorded, along with the known concentration differences between pairings, provided the proportionality constants with which the adjusted concentrations were estimated. The counting of the shifts was facilitated by the use of the Jarrell-Ash microphotometer available. The technique involved can be found in the Ph.D. dissertation of Hsueh.[15] The data for the adjusted concentrations are presented in Table 11.

The criterion used in deciding on the validity of the fringe patterns (i.e., whether the boundary recorded in terms of these shifts

was valid or not within the diffusion time span) had to do with checking whether the shifts were vertical at the upper and lower edges of the transparencies. In all instances, the fringe pattern recorded passed this test quite well.

Evidently, by looking at the values of ϵ_2 in table 11, the crude scheme employed in the preparation of the initial silver nitrate solutions, namely, Eq. (34), "paid off" in terms of rendering ϵ_2 small, even in the concentrated regime.

With these values for ϵ_1 and ϵ_2, the expressions in Table 9 were used to compute the values of the two parameters a_B and b_B. The results can be found in Table 12.

Table 11. Estimation of ϵ_2 by Rayleigh Optics.

Run	Δc of pairings in calibration runs, moles/liter	Average number of shifts recorded	K, proportionality constant, moles/liter/shift	Average number of shifts recorded in actual runs	Concentration difference via K, moles/liter	c_i, moles/liter (from table 2)	c_f, moles/liter	ϵ_2
$A_{21,22}$	0.11942 (1.01696 - 0.89754)	52.75	0.00226	3.25	0.00735	1.01698	1.00963	0.01
$A_{41,42}$	0.10999 (0.48790-0.37791)	61.35	0.00179	11.75	0.02103	0.48670	0.46567	0.04
$A_{51,52}$	0.200	117.65	0.00170 (from Milios)	4.0	0.00680	0.09656	0.08976	0.07
$A_{31,32}$	–	–	–	0.0	0.0	0.01229	0.01229	0.00

Table 12. a_B and b_B.

Run	$\epsilon_1+\epsilon_2=\epsilon$	$(1+\frac{3}{4}\epsilon+\frac{1}{80}\epsilon^2)$	a_B	$(1+\frac{1}{4}\epsilon)$	b_B	b_B/a_B
A_{21}	0.06	1.045	55.4212	1.0150	-1.7723	-0.0320
A_{22}	0.04	1.030	55.4201	1.0100	-1.7712	-0.0320
A_{31}	0.22	1.1656	55.3439	1.0550	-1.5757	-0.0285
A_{32}	0.31	1.2337	55.3439	1.0775	-1.5763	-0.0285
A_{41}	0.10	1.0751	55.3701	1.0250	-1.7054	-0.0308
A_{42}	0.13	1.0977	55.3707	1.0325	-1.7065	-0.0308
A_{51}	0.24	1.1807	55.3464	1.0600	-1.6218	-0.0293
A_{52}	0.31	1.2337	55.3465	1.0775	-1.6230	-0.0293

III. 7. The Transference Numbers of NH_4NO_3 Solutions at 25°C

The transference numbers of the ammonium nitrate solutions examined, as a result of a direct application of Eq. (30), are listed in Table 14, following Table 13 which contains a summary of the term FV/It and the parameters that constituted its make-up.

Table 13. The term FV/It.

Run	V, cm^3 (from Table 6)	I, mA (from Table 8)	t, sec (from Table 7)	It, mAsec	$\frac{F}{It}$, $\frac{1}{g\text{-mole}}$	$\frac{FV}{It}$, cm^3/g-mole
A_{21}	0.8058	20.06227	7,916.34	158,819.750	0.60756	0.48957
	0.8920	20.06202	8,745.18	175,445.976	0.54999	0.49059
	0.9479	20.06182	9,298.38	186,542.426	0.51727	0.49032
A_{22}	0.7417	10.09580	14,399.28	145,372.251	0.66376	0.49231
	0.8059	10.09578	15,636.78	157,865.491	0.61124	0.49260
A_{31}	0.6803	0.50564	3,274.98	1,655.961	58.27009	39.64114
	0.7394	0.50564	3,566.76	1,803.497	53.50328	39.56033
A_{32}	0.6565	0.74946	2,129.28	1,595.810	60.46647	39.69624
	0.7335	0.74946	2,375.88	1,780.627	54.19046	39.74870
A_{41}	0.5692	10.15846	5,299.56	53,835.368	1.79237	1.02022
	0.6445	10.15839	6,001.56	60,966.187	1.58273	1.02007
A_{42}	0.5328	14.99756	3,358.80	50,373.805	1.91554	1.02060
	0.6454	14.99752	4,057.68	60,855.137	1.58562	1.02336
A_{51}	0.4602	5.01156	1,728.18	8,660.878	11.14125	5.12720
	0.5607	5.01161	2,104.26	10,545.730	9.14996	5.13038
	0.6435	5.01158	2,420.71	12,131.582	7.95387	5.11832
A_{52}	0.6591	7.51726	1,645.32	12,368.298	7.80164	5.14206
	0.8006	7.51724	1,997.28	15,014.033	6.42685	5.14534
	0.8526	7.51724	2,140.54	16,090.953	5.99672	5.11280

Table 14. Cation transference number data of NH_4NO_3 at 25°C.

Run	$a_B\ c_3/c_o\|_{x=-\infty}$	FV/It (a)	M_e/ρ_e (b)	b_B/a_B (c)	Sum (a)+(b)+(c)	t_+, or t_1
A_{21}	55.4212 (1.97799×10^{-2}) = 1.096226	0.4896	0.0103	-0.0320	0.4679	0.51292
		0.4906	0.0103	-0.0320	0.4689	0.51402
		0.4903	0.0103	-0.0320	0.4686	0.51369
A_{22}	55.4201 (1.97799×10^{-2}) = 1.096204	0.4923	0.0103	-0.0320	0.4706	0.51587
		0.4926	0.0103	-0.0320	0.4709	0.51620
					avg.	= 0.51454
A_{31}	55.3439 (2.26637×10^{-4}) = 0.012543	39.6411	0.0103	-0.0285	39.6229	0.49699
		39.5603	0.0103	-0.0285	39.5421	0.49598
A_{32}	0.012543	39.6962	0.0103	-0.0285	39.6780	0.49768
		39.7487	0.0103	-0.0285	39.7305	0.49834
					avg.	= 0.49725
A_{41}	55.3701 (9.20966×10^{-3}) = 0.509940	1.0202	0.0103	-0.0308	0.9997	0.50979
		1.0201	0.0103	-0.0308	0.9996	0.50974
A_{42}	55.3707 (9.20966×10^{-3}) = 0.509945	1.0206	0.0103	-0.0308	1.0001	0.51000
		1.0234	0.0103	-0.0308	1.0029	0.51142
					avg.	= 0.51024
A_{51}	55.3464 (1.79567×10^{-3}) = 0.099384	5.1272	0.0103	-0.0293	5.1082	0.50767
		5.1304	0.0103	-0.0293	5.1114	0.50799
		5.1183	0.0103	-0.0293	5.0993	0.50679
A_{52}	55.3465 (1.79567×10^{-3}) = 0.099384	5.1421	0.0103	-0.0293	5.1231	0.50915
		5.1453	0.0103	-0.0293	5.1263	0.50947
		5.1128	0.0103	-0.0293	5.0938	0.50624
					avg.	= 0.50789

The standard deviations and uncertainties involved with the data in Table 14 are presented in Table 15. The former measure was taken to be the collective contributions of the variables I, t, and V. The uncertainty brought about by the presence of the term

$$\left.\frac{c_3}{c_o}\right|_{x=-\infty}$$

was assumed to be that due to the weight of salt, an absolute value of 0.001 gram. The sum of the uncertainties, and their absolute amounts, are reproduced in the following table for easy reference.

Table 15. The transference numbers and their uncertainties.

Run	Average t_1	Standard deviation	% uncertainty	% uncertainty (salt)	sum	t_1, complete
$A_{21,22}$	0.51454	±0.00141	0.274	0.001	0.275	0.5145±0.0014
$A_{31,32}$	0.49725	±0.00105	0.211	0.089	0.300	0.4973±0.0015
$A_{41,42}$	0.51024	±0.00077	0.151	0.003	0.154	0.5102±0.0008
$A_{51,52}$	0.50789	±0.00127	0.250	0.015	0.265	0.5079±0.0014

III.8. The Transference Numbers of $AgNO_3$ Solutions at 25°C

The fringe shifts recorded for the concentration boundaries, when manipulated correctly, yielded the concentrations of the adjusted following solutions,

$$c_3\big|_{x=+\infty}$$

(see Table 16). With the literature equation for the density function at hand, Eq. (35), densities for these adjusted solutions were obtained. They, in turn, generated

$$c_o\big|_{x=+\infty} \quad .$$

The Kohlrausch regulating function was finally made use of in calculating for the transference numbers of the following cations, i.e., t_{Ag^+}.

Table 16. The calculated t_{Ag^+}'s.

Run	$c_f=c_3\big\|_{x=+\infty}$ moles/liter	ρ,gm/ml	$c_o\big\|_{x=+\infty}$ moles/liter	$\frac{c_3}{c_o}\big\|_{x=+\infty}$	$\frac{c_3/c_o\big\|_{x=+\infty}}{c_3/c_o\big\|_{x=-\infty}}$	t_2
$A_{21,22}$	1.0096	1.137753	53.632	0.018825	0.9517	0.490
$A_{31,32}$	0.0123	0.998816	55.325	0.000222	0.9797	0.487
$A_{41,42}$	0.4657	1.062356	54.576	0.008533	0.9265	0.473
$A_{51,52}$	0.0898	1.009752	55.201	0.001627	0.9061	0.460

As can be seen, the value for t_2 at the very dilute concentration of 0.0123M is not reasonable. This is not surprising, as the Rayleigh system, with the 9mm interference cell assembly incorporated in it, is incapable of detecting the faint concentration boundary actually present. Irregardless of the setting of the inclination of the analyzer diaphragm,

the multiple slit for the Rayleigh system contained only a finite (162) number of point sources of finite width and separation distance from one another. Evidently, the minute concentration difference in this very dilute solution exceeded the degree of accuracy, order-of-magnitude-wise, available in the Perkin-Elmer apparatus for the detection of concentration differences in the dilute regime.

Therefore, for this concentration, the only outcome takes the form of the leading ion transference number. The small and nonsharply-outlined Schlieren peak recorded (with the analyzer diaphragm set at its acutest angle of inclination) did not, however, in any way affect adversely the microphotometer intensity analysis administered to the transparencies containing it.

This writer feels compelled to note here that in runs involving solutions of concentrations equal to about 0.5M and above (i.e., runs $A_{21,22,41,42}$, and the 2M runs discussed later), even with the analyzer slit set to yield the most distinct peak outlines, the peak apexes did not present themselves on film. Rather, a thick dark band occupied the whole lateral area between the two peak slopes quite symmetrically (cf. figure 7). This phenomenon was present in the Rayleigh combination transparencies as well as in pictures taken with the cylindrical lens removed (i.e., pictures that showed just the 2mm width marked cell channel). In general, the thickness of the dark band grew, qualitatively speaking, as the solutions became more concentrated.

The presence of the dark band notwithstanding, the two symmetrical (as far as the naked eye could tell), curving portions of the peaks recorded were distinct enough (they were separated from the thick band

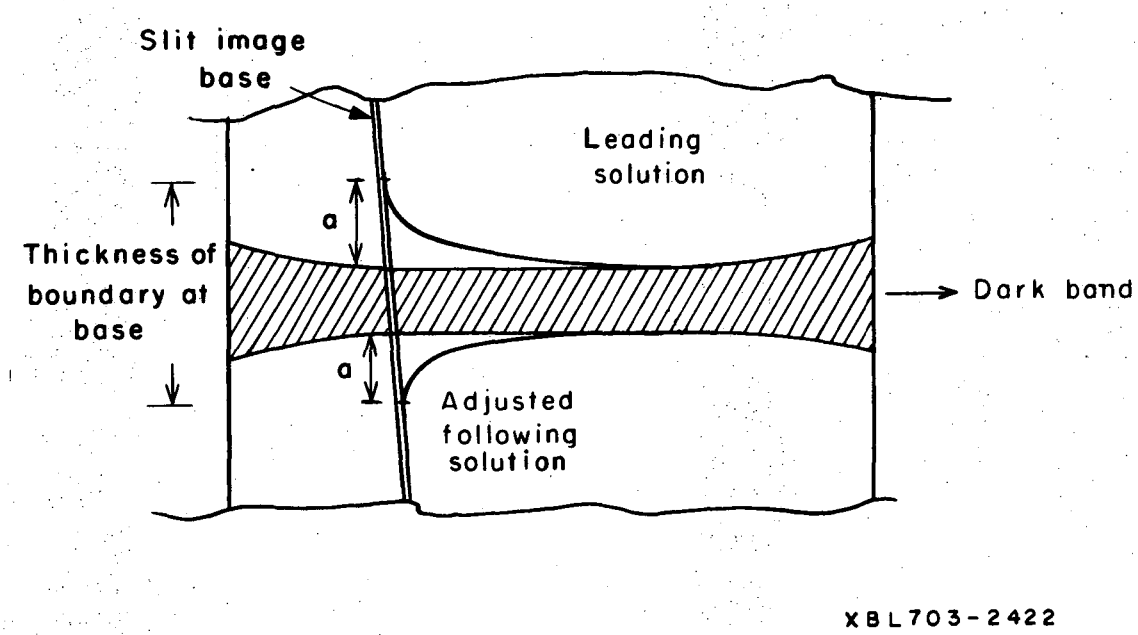

Fig. 7. Schematic sketch of a Schlieren peak in solutions with $c \gtrsim 0.5$ M.

sufficiently) that the microphotometer analysis technique (as presented in Section III.3 (b) (iii)) of locating the absolute position of the peak as the mid-point of the two intensity peaks formed by these curves met with no difficulties. As far as the analysis went, it mattered not at all whether indeed there was an apex to a Schlieren peak or not; the crucial question was one of lateral peak symmetry, and this was observed to be present in all cases experienced.

This experimenter had on three occasions attempted runs with a 2M NH_4NO_3 solution (2.00467M to be exact) and two slightly less concentrated $AgNO_3$ solutions (1.95917M and 1.96142M). In one instance with the first of the latter as the following solution, there was a heretofore unobserved, significant electrical phenomenon present while the run was progressing, with the result that the current could not be held reasonably stationary (drifts in the current were always present to a controllable degree in all the other runs in the present work)within the voltage scale set on the chart recorder. This was, hoever, the lesser of two adversities, and was absent in the other two runs, most probably because whatever system leakage or incompatibility involved was removed by one of the several leakage-prevention measures elaborated upon earlier. The major problem observed was one in which the bottom portion of the Schlieren peak was distorted weirdly in the region immediately below the lower edge of the dark band. The negatives taken with the cylindrical lens out of the optical system showed that immediately below the lower edge of the now 2 mm wide dark band a streak of exceptional bright light covered the width of the channel. This streak was less prominent in

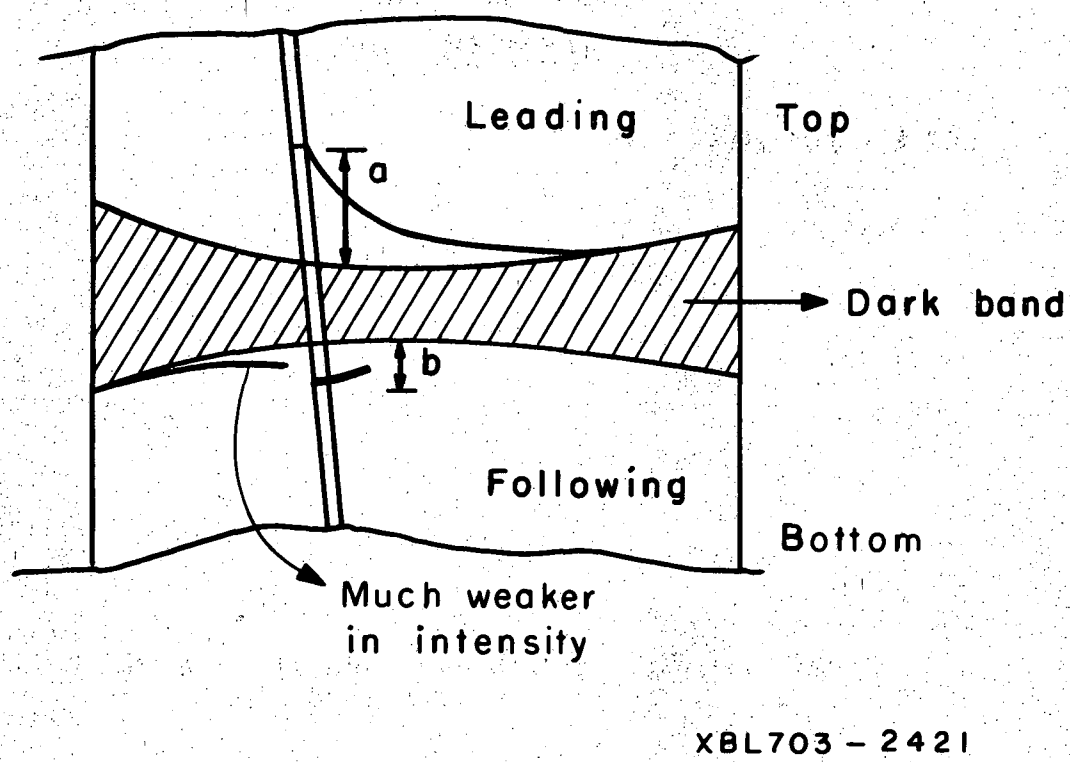

Fig. 8. A sketch of the distorted Schlieren peak phenomenon.

brightness in the Rayleigh and Schlieren pictures. But immediately beneath it in the photographs with the Rayleigh combination phenomenon whatever fringes might have been present could not be distinctly made out, whereas in the leading solution region on top of the band the vertical fringes were both clear and distinct (as in the other runs with less concentrated ammonium and silver nitrates). Further down the transparency they became a little clearer, although a far cry from the norm in terms of distinctiveness and verticalness, as they were slanted from the vertical and there were indications of fringe-batch overlaps. The bottom curving portion of the peak (as evidenced in the Rayleigh and Schlieren transparencies), a much weaker intensity-wise and narrower version than its counterpart on top, seemingly was dissected somewhere after it began its sloping toward the dark band that was in the center portion of what was taken to be that of the lateral peak, as depicted in figure 8. Furthermore, distance b is less than distance a. It was reasoned after such a run that perhaps the blame was with the following solution. Consequently, another $AgNO_3$ solution was made up (1.96142M); its concentration came closer to the leading ion concentration. Another run was made, and it was again observed that with everything else involved in good order the above phenomenon did not vanish. Besides, the dark band in these three runs had become menacingly thick; distance a was not "large" enough to command comfort and contentment (drawn out-sized in Fig. 8 for illustrative purposes). As this writer had not the necessary expertise in optics (one possible answer for the above discrepancies) or the time to try to secure it (largely due to his own tardiness), the problem was left, rather

grudgingly, undisturbed. The abnormalities destroyed any hope of pinpointing the moving boundary location, and at the same time locating the concentration boundary in its wake.

It is entirely possible that the following solution concentration becomes critical, in its relationship with the leading solution concentration in the concentrated regime. It is more probable, however, that the real problem lies with the optical make-up of the present system, although this writer would be very much remiss if he were to claim that he had a valid argument to support this statement. It had been suggested that perhaps the 9 mm length of the optical channel could be reduced somewhat to entertain these aberrations, but whether this would in reality rise to the occasion in solving the problem or would fail in its attempt could not be ascertained at the moment.

It was noted in general that the thickness of the boundary at its base increases proportionately as the quantity of current passed decreased, for the same pair of NH_4NO_3-$AgNO_3$ solutions tested. As noted by Milios and Newman,[9] this relationship can be theoretically supported. In all instances, the current direction was such that roughly speaking,

$$z_1 i t_1 < z_2 i t_2 \tag{36}$$

i.e., the leading solution had the higher conductivity, as the boundaries obtained during runs were stable.

Haase, et al.,[4] have reported data on the Ag^+ transference number as a function of concentration using a Lewis-type[2,16] volume correction model. In the context of the present two-salt system, the equation for

the transference number of, say, the leading ion, in the Lewis form is the following,

$$t_1^L = \frac{-z_3c_3\big|_{x=-\infty}}{1-c_3\big|_{x=-\infty}\bar{V}_A^H}\left[\frac{FV}{It} + \frac{\bar{V}e}{z_2} - \frac{\bar{V}_B^H}{z_2\nu_2}\right] \tag{37}$$

$$= -\frac{z_3c_3\big|_{x=-\infty}}{c_o\big|_{x=-\infty}\bar{V}_{oA}^H}\left[\frac{FV}{It} + \frac{\bar{V}e}{z_2} - \frac{\bar{V}_B^H}{z_2\nu_2}\right] \tag{38}$$

It has been shown[1] that

$$\frac{t_1^L}{t_1} = \frac{a_A}{a_B} = \frac{\bar{V}_{oB}}{\bar{V}_{oA}} \tag{39}$$

where a_A is given by an expression that is analogous to equation (14).

In the case where the partial molal volume of the solvent is constant through the moving boundary, therefore, these two transference number equations become one and the same. The conversion of the Haase numbers to the present, more rigorous system, in the manner introduced by Milios[19] in consultation with Newman, involves the following scheme.

Equation (21), when cast in another light, becomes

$$t_1 = -a_B\frac{z_3c_3}{c_o}\bigg|_{x=-\infty}\left[\frac{FV}{It} + \frac{\bar{V}_e}{z_2} + \frac{b_B}{z_2\nu_2a_B}\right] \tag{40}$$

The connection between Eqs. (38) and (40) is immediately obvious, with the result that

$$t_1 = a_B \frac{(1-c_3|_{x=-\infty}\bar{V}_A^H)}{c_o|_{x=-\infty}} t_1^L - \frac{z_3 c_3|_{x=-\infty}}{z_2 \nu_2 c_o|_{x=-\infty}}(a_B \bar{V}_B^H + b_B) \qquad (41)$$

In Haase's endeavor, "B" refers to $Cu(NO_3)_2$ and is the following solution to $AgNO_3$, and ion 2 represents the Cu^{++} ion. Hence $z_2 = 2$ and $\nu_2 = 1$. Since $\bar{V}_A^H$ and $\bar{V}_B^H$ are known as 0.02801 and 0.03270 ml/gmole, respectively, the task becomes one of ascertaining the values of a_B and b_B.

From a linear plot of the density data of $Cu(NO_3)_2$ (the data presented in Haase's paper) from 0.0 to 0.7 M concentration (the linear plot fits the data exceedingly well, as pointed out by Milios), Milios was able to formulate the following equation for the concentration of the solvent,

$$c_o|_{x=-\infty} = 55.3421 - 1.90c_3|_{x=-\infty} \quad , \quad 0 < c < 0.7 \text{ M} \quad . \qquad (42)$$

$$= a_B + b_B c_3|_{x=-\infty} \qquad (43)$$

Also,

$$\rho_{AgNO_3} \text{ at } 25°C = 0.997074 + 0.141956c_3|_{x=-\infty} - 0.002603c_3^{3/2}|_{x=-\infty} \qquad (44)$$

$$= \frac{18.016\ c_o|_{x=-\infty} + 169.888c_3|_{x=-\infty}}{1000}$$

With the above information, and the assumption that Haase's following solutions had concentrations within the above range, conversions were effected. The results are shown in Table 17.

Table 17. t_{Ag^+}, a comparison.

$c_3\|_{x=+\infty}$ concentration of Ag^+ moles/liter (present analysis)	$c_3\|_{x=-\infty}$ concentration of Ag^+ moles/liter (Haase, et al.[4])	$c_o\|_{x=-\infty}$ solvent conc., moles/liter (Haase)	$t^L_{Ag^+}$ (Haase)	t_{Ag^+} (Haase corrected)	t_{Ag^+} (present)
0.0898					0.460±0.009
	0.09962	55.1848	0.4687	0.4686	
			0.4676	0.4675	
			0.4674	0.4673	
				avg=0.4678	
0.1950 (Milios')					0.467±0.009
	0.1995	55.0216	0.4723	0.4722	
			0.4708	0.4707	
				avg=0.4715	
0.4657					0.473±0.010
	0.4995	54.5184	0.4819	0.4819	
			0.4812	0.4812	
				avg=0.4816	
	0.9978	53.6529	0.4953	0.4958	
1.0096					0.490±0.010
	1.1005	53.4708	0.5007	0.5011	

It should be noted that the indirect results for t_{Ag^+} (present) from the Kohlrausch regulating function, due to the uncertainties in the weight of $AgNO_3$ salt (i.e., $c_{3|x=+\infty}$) and in $t_{NH_4^+}$, are accurate only to about 2%. As can be observed from Table 17, the data agree reasonably well with one another. It is interesting to note also that the conversions have only affected the fourth decimal place of some of the Haase numbers.

III. 9. Summary of the transference number data for NH_4NO_3 at 25°C

Since the literature datum[18] available for ammonium nitrate solutions has been obtained via a Lewis-type volume correction procedure, and the present analysis yields numbers via a Milios-type formulation, it is felt that a comparison of the two sets can be effected only after the necessary conversions have been made. The lack of relevant data concerning the particular partial volumes and density function involved with this only other transference number (than the one at infinite dilution) reported has prompted this writer to go the other way, so to speak, and convert the present numbers to the Lewis scheme, just for interest's sake.

The presence of Eq. (39) makes it all possible. With the introduction of an equation for the solvent partial molal volume in a single salt solution (subscripted i) at hand, in the fashion initiated by Milios[1] in Appendix B of his thesis,

$$\bar{V}_{oi} = \frac{M_o}{\rho_i - c_i \frac{\partial \rho_i}{\partial c_i}} \quad , \qquad (45)$$

and the literature density equations for NH_4NO_3(A) and Ag NO_3(B) at 25°C,

$$\rho_A = 0.997077 + 0.032628c_A - 0.000963c_A^{3/2} - 0.0000473c_A^2 \tag{46}$$

and

$$\rho_B = 0.997074 + 0.141956c_B - 0.002603c_B^{3/2} \quad , \tag{47}$$

one can arrive at the following,

$$\overline{V}_{oA} = \frac{M_o}{0.997077 + 0.0004815c_A^{3/2} + 0.0000473c_A^2} \tag{48}$$

and

$$\overline{V}_{oB} = \frac{M_o}{0.997074 + 0.0013015c_B^{3/2}} \tag{49}$$

It follows, then, that

$$\frac{t_1^L}{t_1} = \frac{0.997077 + 0.0004815c_3^{3/2}\Big|_{x=-\infty} + 0.0000473c_3^2\Big|_{x=-\infty}}{0.997074 + 0.0013015c_3^{3/2}\Big|_{x=+\infty}} = \frac{\overline{V}_{oB}}{\overline{V}_{oA}} \tag{50}$$

from which the conversion from t_1 to t_1^L can be facilitated. The calculations culminate in Table 18.

Table 18. The conversion from t_1 to t_1^L.

Run	$c_3\|_{x=-\infty}$ moles/liter	$c_3\|_{x=+\infty}$ moles/liter	t_1	$\bar{V}_{oB}$ cm^3/mole	$\bar{V}_{oA}$ cm^3/mole	$\frac{\bar{V}_{oB}}{\bar{V}_{oA}}$	t_1^L
$A_{21,22}$	1.039406	1.0096	0.5145	0.997638	0.998394	0.9992	0.5141
$A_{31,32}$	0.012536	0.0123	0.4973	0.997084	0.997076	1.0000	0.4973
$A_{41,42}$	0.497462	0.4657	0.5102	0.997258	0.997488	0.9998	0.5101
$A_{51,52}$	0.098909	0.0898	0.5079	0.997092	0.997109	1.0000	0.5079

All the pertinent t_1 data are summarized in Table 19.

Table 19. Summary of $t_{NH_4^+}$ at 25°C.

$c_3\|_{x=-\infty}$ moles/liter	t_1	t_1^L	Source
0.00	0.5072	0.5072	Arrived at analytically via a consideration of limiting ionic mobilities--ref. (17)
0.0125	0.4973±0.0015	0.4973	Present analysis
0.0989	0.5079±0.0014	0.5079	Present analysis
0.10		0.5130	MacInnes and Cowperthwaite - ref.18
0.2131	0.5140±0.0025	0.5139	Milios - ref. (1)
0.4975	0.5102±0.0008	0.5101	Present analysis
1.0394	0.5145±0.0014	0.5141	Present analysis

As can be seen, the distinction between the Lewis and the Milios approaches, as brought out in the above manner, is not readily noticeable, except, perhaps, at higher concentrations. Even so, the difference is only in the fourth decimal place of the data, and this finding might be coupled with a similar one in the other conversion direction (see Table 17 and subsequent discussions) to indicate that the ratio of solvent partial molal volumes through a two-salt moving boundary is not appreciably different from unity, for concentrations about 1.0 M and less. The table does point out that the fourth and fifth numbers deviate noticeably from the general trend of the others, and they are precisely those that did not originate from the present endeavor. It is not immediately obvious why this is the case.

IV. Conclusions

The moving-boundary expression for the transference number as derived by Milios[1] in conjunction with Newman, and the experimental technique fashioned by the former, together yield the following data for the NH_4NO_3-$AgNO_3$ system at 25°C.

Table 20. $t_{NH_4^+}$ and t_{Ag^+}.

$c_3\|_{x=-\infty}$ moles/liter	t_1	$c_3\|_{x=+\infty}$ moles/liter	t_2
0.0125	0.4973±0.0015	0.0123	--
0.0989	0.5079±0.0014	0.0898	0.460±0.009
0.4975	0.5102±0.0008	0.4657	0.473±0.010
1.0394	0.5145±0.0014	1.0096	0.490±0.010

The chief aim in the present endeavor has been to find these numbers. The next logical step of theoretical interpretations is left undone. It might be said that the one regret felt in the course of this brief experience in the laboratory stems from the inability to discover other numbers characteristic of solution concentrations of a higher order. The technical barriers have been alluded to earlier, and will not be re-iterated here. It suffices to say that the present effort has been successful in terms of its objective within a concentration range of between 0.0125 M and 1.0394 M in ammonium nitrate, and 0.0898 M and 1.0096 M in silver nitrate.

This writer feels compelled to inject, as a parting shot, an aspiration of sorts for a time-measuring device that automatically punches

out time-intervals whenever desired. In terms of his experience with the monitoring of the time variable, the inclusion of such a piece of equipment would be a definite improvement as well as a competent soother of nerves.

V. Acknowledgments

I would like to express my gratitude to Professor John Newman for his encouragement and guidance in this project. I would also like to express my deep appreciation for my wife, Margaret, for all that she has done to motivate me toward accomplishing the task before me. My thanks also go to Jacqueline Cross for typing the final manuscript.

This work was done under the auspices of the United States Atomic Energy Commission.

Nomenclature

a_I	defined by equations (14) and (42)
A	cross-sectional area of cell channel, cm^2
A	surface area of electrode, cm^2
b_I	defined by equations (14) and (42)
c_i	concentration of species i, $moles/cm^3$
c_T	total solution concentration, $moles/cm^3$
$c_{initial}$	lowest concentration of following solution removed from the two-salt boundary, $moles/cm^3$
c_{final}	highest concentration of following solution removed from the two-salt boundary, $moles/cm^3$
D	diffusion coefficient, cm^2/sec
$\mathcal{D}_{ij}$	diffusion coefficient for binary interactions, cm^2/sec
e	defined by equations (24) and (25)
f	defined by equations (24) and (25)
F	Faraday's constant, 96,493 coul/equivalent
g	defined by equations (24) and (25)
g	acceleration of gravity, cm/sec^2
h	defined by equations (24) and (25)
i	current density, $Amps/cm^2$
I	current, Amps
k_1, k_2, k_3, k_4	defined by equation (22)
L	electrode height, cm
M	molarity of solution, moles/liter
M_I	molecular weight of substance I, gm/mole

R	universal gas constant, joule/mole-deg
t	time, sec
t_i	transference number of species i
t_i^L	transference number of species i as calculated using a Lewis-type volume correction, see equation (37)
T	temperature, deg K
v_b	velocity of the two-salt boundary, cm/sec
v_i	velocity of species i, cm/sec
V	volume through which the two-salt boundary moves, cm^3
V	volume, cm^3
$\bar{V}_I$	partial molal volume of substance I, cm^3/mole
x	distance variable, cm
z_i	charge number of species i
α_I	defined by equation (12)
β	coefficient of expansion, $(1/\rho)(\partial\rho/\partial c)$, see equation (28), cm^3/mole
β_I	defined by equation (12)
ϵ	$= (c_{final} - c_{initial})/c_{initial}$
ϵ_1	contribution to ϵ due to electrode reaction
ϵ_2	contribution to ϵ due to presence of concentration boundary caused by Kohlrausch regulating function
μ_i	electrochemical potential of species i, joule/mole
ν	kinematic viscosity, cm^2/sec
ν_+	number of cations produced by the dissociation of one molecule of electrolyte
ρ_e	density of electrode material, gm/cm^3

ρ_I	density of solution I, gm/cm^3, gm/liter in equation (13)

Subscripts

0	solvent
1	leading ion when boundary rises, following ion when boundary falls
2	following ion when boundary rises, leading ion when boundary falls
3	common ion
b	two-salt boundary
e	electrode
∞	far removed
$x=-\infty$	evaluated in solution A at concentration required by the Kohlrausch relation
$x=+\infty$	evaluated in solution B at concentration required by the Kohlrausch relation
A	salt or salt solution composed of ions 1 and 3
B	salt or salt solution composed of ions 2 and 3
+	cation
-	anion

Superscripts

B	salt solution composed of ions 2 and 3
H	associated with Haase *et al.*[4]
L	associated with a Lewis-type[2,16] volume correction

References

1. Milios, Paul, M.S. Thesis, University of California, Berkeley, 1967 (UCRL-17807).

2. MacInnes, D. A., and L. G. Longsworth, Chem. Revs., 31, 171 (1932).

3. Bearman, R. J., J. Chem. Phys., 36, 2432 (1962).

4. Haase, R., G. Lehnert, and H.-J. Jansen, Zeit. für Phys. Chem., N. F. 42, 32 (1964).

5. Tamás, J., O. Kaposi, and P. Scheiber, Acta. Chim. Acad. Sci. Hung., 48 (4), 309 (1966).

6. Kaimakov, E. A., and N. L. Varshavskaya, Russ. Chem. Revs., 35 (2), 89 (1966).

7. Chapman, T. W., and John Newman, "A Compilation of Selected Thermodynamic and Transport Properties of Binary Electrolytes in Aqueous Solution," UCRL-17767, 1968.

8. Weber, H., Sitz, Deut. Akad. Wiss. Berlin, 936 (1897); Weber, H., "Die Partiellen Differential-gleichungen der Mathematischen Physik," Friedrich Vieweg und Sohn, Braunschweig, 1900, pp. 481-506.

9. Milios, Paul and John Newman, J. Phys. Chem., 73, 298 (1969).

10. Longsworth, L. G., J. Am. Chem. Soc., 66, 449 (1944).

11. Chapman, T. W., Ph.D. Thesis, University of California, Berkeley, 1967 (UCRL-17768).

12. Tiselius, A., Trans. Far. Soc., 33, 524 (1937).

13. Campbell, A. N., A. P. Gray, and E. M. Kartzmark, Can. J. Chem., 31 617 (1953).

14. Smithsonian Physical Tables, 9 ed., Rev., Table 291, Washington, D.C., 1954, reproduced in Perry's Chemical Engineers' Handbook, 4 ed., 3-71, Table 3-47.

15. Hsueh, Limin, Dissertation, University of California, Berkeley, January, 1969 (UCRL-18597).

16. Lewis, G. N., J. Am. Chem. Soc., 32, 862 (1910).

17. Milazzo, G., "Electrochemistry", Elsevier Publishing Co., Amsterdam, 1963.

18. MacInnes, D. A., and I. A. Cowperthwaite, Trans. Far. Soc., 23, 400 (1927).

19. Milios, Paul, private communication through Professor John Newman, May, 1969.

Source Material

1. Newman, John. "Transport Processes in Electrolytic Solutions," Advances in Electrochemistry and Electrochemical Engineering, 5, 87-135(1967).

2. Smits, L. J. M., and E. M. Duyvis. "Transport Numbers of Concentrated Sodium Chloride Solutions at 25°C." The Journal of Physical Chemistry, 70, 2747-2753 (1966).

3. Spiro, M. "Volume Correction for the Indirect Moving-Boundary Method and the Transference Numbers of Concentrated Aqueous Sodium Chloride Solutions." The Journal of Chemical Physics, 42, 4060-4061 (1965).

4. Longsworth, L. G. "A Differential Moving Boundary Method for Transference Numbers." The Journal of the American Chemical Society 65, 1755-1765 (1943).

5. Longsworth, L. G. "A Modification of the Schlieren Method for Use in Electrophoresis Analysis." ibid., 61, 529-530 (1939).

6. Longsworth, L. G. "Moving Boundary Electrophoresis-Theory." (Chapter 3) and "Moving Boundary Electrophoresis-Practice." (Chapter 4), in Electrophoresis, M. Bier, editor, Academic Press, Inc., New York, 1959.

7. Bearman, R. J. "Further Consideration of the Moving Boundary Experiment for the Measurement of Transference Numbers." To be submitted to The Journal of Physical Chemistry.

8. Muller, R. H. "Optical Techniques for the Study of Diffusional Mass Transfer." UCRL-11542 (unpublished), July, 1964.

LEGAL NOTICE

This report was prepared as an account of Government sponsored work. Neither the United States, nor the Commission, nor any person acting on behalf of the Commission:

A. Makes any warranty or representation, expressed or implied, with respect to the accuracy, completeness, or usefulness of the information contained in this report, or that the use of any information, apparatus, method, or process disclosed in this report may not infringe privately owned rights; or

B. Assumes any liabilities with respect to the use of, or for damages resulting from the use of any information, apparatus, method, or process disclosed in this report.

As used in the above, "person acting on behalf of the Commission" includes any employee or contractor of the Commission, or employee of such contractor, to the extent that such employee or contractor of the Commission, or employee of such contractor prepares, disseminates, or provides access to, any information pursuant to his employment or contract with the Commission, or his employment with such contractor.

TECHNICAL INFORMATION DIVISION
LAWRENCE RADIATION LABORATORY
UNIVERSITY OF CALIFORNIA
BERKELEY, CALIFORNIA 94720